

See discussions, stats, and author profiles for this publication at: <https://www.researchgate.net/publication/265059067>

# Identification of Multiple Cellular Uptake Pathways of Polystyrene Nanoparticles and Factors Affecting the Uptake: Relevance for Drug Delivery Systems

ARTICLE *in* EUROPEAN JOURNAL OF CELL BIOLOGY · AUGUST 2014

Impact Factor: 3.83 · DOI: 10.1016/j.ejcb.2014.08.001

---

CITATIONS

2

READS

86

---

## 3 AUTHORS, INCLUDING:



[Rebuma Firdessa](#)

University of Wuerzburg

18 PUBLICATIONS 273 CITATIONS

[SEE PROFILE](#)



[Tobias Oelschlaeger](#)

University of Wuerzburg

20 PUBLICATIONS 516 CITATIONS

[SEE PROFILE](#)



Contents lists available at ScienceDirect

# European Journal of Cell Biology

journal homepage: [www.elsevier.com/locate/ejcb](http://www.elsevier.com/locate/ejcb)



## Identification of multiple cellular uptake pathways of polystyrene nanoparticles and factors affecting the uptake: Relevance for drug delivery systems

Rebuma Firdessa, Tobias A. Oelschlaeger, Heidrun Moll\*

Institute for Molecular Infection Biology, University of Würzburg, Würzburg, Germany

### ARTICLE INFO

#### Article history:

Received 15 May 2014

Received in revised form 12 August 2014

Accepted 12 August 2014

#### Keywords:

Nanoparticle

Ultrastructure

Endocytosis

Multiple uptake

Factor determining uptake

### ABSTRACT

Nanoparticles may address challenges by human diseases through improving diagnosis, vaccination and treatment. The uptake mechanism regulates the type of threat a particle poses on the host cells and how a cell responds to it. Hence, understanding the uptake mechanisms and cellular interactions of nanoparticles at the cellular and subcellular level is a prerequisite for their effective biomedical applications. The present study shows the uptake mechanisms of polystyrene nanoparticles and factors affecting their uptake in bone marrow-derived macrophages, 293T kidney epithelial cells and L929 fibroblasts. Labeling with the endocytic marker FM4-64 and transmission electron microscopy studies show that the nanoparticles were internalized rapidly via endocytosis and accumulated in intracellular vesicles. Soon after their internalizations, nanoparticles trafficked to organelles with acidic pH. Analysis of the ultrastructural morphology of the plasma membrane invaginations or extravasations provides clear evidence for the involvement of several uptake routes in parallel to internalize a given type of nanoparticles by mammalian cells, highlighting the complexity of the nanoparticle-cell interactions. Blocking the specific endocytic pathways by different pharmacological inhibitors shows similar outcomes. The potential to take up nanoparticles varies highly among different cell types in a particle size-, time- and energy-dependent manner. Furthermore, infection and the activation status of bone marrow-derived macrophages significantly affect the uptake potential of the cells, indicating the need to understand the diseases' pathogenesis to establish effective and rational drug-delivery systems. This study enhances our understanding of the application of nanotechnology in biomedical sciences.

© 2014 Elsevier GmbH. All rights reserved.

## Introduction

Many diseases originate from alterations in biological processes that result from mutated genes, misfolded proteins, and infections caused by pathogens at the molecular or nanoscale level (1–100 nm) (Kim et al., 2010). These molecules and infectious agents are nanometers in size and their chemical properties, size and shape appear to dictate their transport to distinct cellular

compartments and the interactions between the molecules (Kim et al., 2010). Nanoparticles (NPs) are similar in scale to these biological molecules or agents and can be engineered due to their unique physical and chemical properties to be used for diagnosis, vaccination and treatment of diseases at the molecular level. This can be achieved through encapsulating, covalently attaching or adsorbing molecules on such NPs to overcome biomedical pitfalls including sensitivity of diagnostic tools, therapeutic effectiveness, toxicity and side effects of drugs, and immunogenicity of vaccines (Briones et al., 2008; Karve et al., 2012; Li et al., 2011). Among these various applications, the development of medicines containing NP suspensions has made it possible to increase the therapeutic index of many components by selectively directing them toward the diseased tissues and cells, leading to medical breakthroughs (Couvreur, 2013; Karve et al., 2012). So far, NP-based chemotherapeutics for six cancer and more than 11 other diseases have been approved for clinical use and many more are being studied in clinical trials (Wang et al., 2012). For such a wide range of NP applications in medicine, understanding their uptake mechanisms and interactions at the cellular

**Abbreviations:** BMDM, bone marrow-derived macrophages; CpG ODN, oligodeoxynucleotides containing unmethylated cytosine-phosphate-guanine; DMEM, Dulbecco's Modified Eagle Medium; RPMI, Roswell Park Memorial Institute; FACS, fluorescence-activated cell sorter; MFI, mean fluorescence intensity; NP, nanoparticle; PBS, phosphate-buffered saline; RT, room temperature; TEM, transmission electron microscopy.

\* Corresponding author at: Institute for Molecular Infection Biology, University of Würzburg, Josef-Schneider-Street 2/D15, D-97080 Würzburg, Germany.

Tel.: +49 931 3182627; fax: +49 931 3182578.

E-mail address: [heidrun.moll@uni-wuerzburg.de](mailto:heidrun.moll@uni-wuerzburg.de) (H. Moll).

<http://dx.doi.org/10.1016/j.ejcb.2014.08.001>

0171-9335/© 2014 Elsevier GmbH. All rights reserved.

and subcellular level is a prerequisite and currently an active area of research because the route of uptake is critical for the intracellular fate of the particles and the induction of biological responses ([Kumari et al., 2010](#); [Scita and Di Fiore, 2010](#)). However, the mechanism(s) of NP-cell interactions are still not fully understood and it has been suggested that the accurate knowledge of NP uptake mechanisms is an important criterion to progress in the field of nanomedicine ([Chou et al., 2011](#); [Iversen et al., 2011](#); [Yan et al., 2012](#)).

Over the past years, considerable numbers of studies have been conducted to understand the route through which NPs are taken up by different cells. The results indicate that NP entry takes place through endocytosis mechanisms operating in mammalian cells ([Chou et al., 2011](#); [Iversen et al., 2011](#)). These distinct endocytic pathways have been characterized on the basis of their differences in ultrastructure, pharmacology, cargo (membrane protein, or receptor plus ligand) and coat protein composition ([Hansen and Nichols, 2009](#); [Sandvig et al., 2011](#); [Xu et al., 2013](#)). The ultrastructural morphology of nascent endocytic intermediates at the plasma membrane provides a crucial parameter for classifying endocytic pathways ([Hansen and Nichols, 2009](#)). Typically, endocytosis occurs by multiple mechanisms that fall into two broad categories: 'Phagocytosis' or cell eating by which cells internalize large solid particles, and 'pinocytosis' or cell drinking, where cells take up both fluid and solutes from their environment. Pinocytosis can be further sub-classified and at least four basic mechanisms can be distinguished: macropinocytosis, clathrin-mediated endocytosis, caveolae-mediated endocytosis, and clathrin- and caveolae-independent pathways ([Conner and Schmid, 2003](#); [Yan et al., 2012](#)). The identification of several uptake routes and pathways complicates the study of the cellular uptake of NPs. Furthermore, these uptake mechanisms of NPs have been shown to be highly influenced by the physicochemical properties of NPs including size, surface functionalization, geometry and other factors like concentration, time or cell types ([Albanese et al., 2012](#); [Dos Santos et al., 2011](#); [Herd et al., 2013](#); [Saha et al., 2013](#)) making the comparison of different findings even more difficult. In multicellular organisms, the distinct endocytic pathways are highly regulated to control all aspects of intercellular communications including hormone-mediated signal transduction, immune surveillance, antigen presentation, and cellular and organismal homeostasis ([Conner and Schmid, 2003](#); [Sanjuan et al., 2007](#); [Underhill and Goodridge, 2012](#)). As a result, one of the goals of designing NP-based delivery systems is to be able to correlate uptake routes with the physicochemical properties of the engineered NPs in order to guide the entry into the cell and, consequently, control the cellular responses. For example, [Karlsson et al. \(2013\)](#) described that bone marrow-derived dendritic cells use caveolin-dependent pathways to take up 40–50 nm polystyrene NPs. Thus, unlike most other NPs, they do not induce extracellular signal-regulated kinases that mediate inflammatory pathways during their applications in vaccines. Furthermore, it has been suggested that alterations in the physicochemical properties of nanomaterials can regulate uptake mechanisms and the intracellular fate of NPs ([Herd et al., 2013](#); [Saha et al., 2013](#); [Yan et al., 2012](#)). However, there is little consensus in the literature regarding this issue. For instance, [Rejman et al. \(2004\)](#) studied size-dependent internalization of particles and concluded that microspheres of greater size (>500 nm) predominantly involve caveolae-dependent endocytosis. On the other hand, [Yan et al. \(2012\)](#) found that caveolae pathways are generally limited to smaller (<150 nm) materials. Moreover, [Fernando et al. \(2010\)](#) suggested that the cellular uptake of 18 ( $\pm$ 5) nm size polymer NPs occurs via constitutive macropinocytosis rather than clathrin-dependent or caveolin-dependent mechanisms. Importantly, it has not yet been fully resolved whether a single cell or cell type uses several uptake pathways simultaneously for a given nanomaterial

or NPs having the same physicochemical properties. In addition to the lack of strict specificity of some pharmacological inhibitors, this might have contributed to the inconsistent results obtained in different studies ([Vercauteren et al., 2010](#)). Furthermore, the effect of infection or the diseases' pathogenesis on the cellular uptake mechanisms of NPs has never been fully investigated.

Moreover, the type of laboratory techniques applied, the variability in fluorescence of some NPs used for tracking, the lack of uniformity in their physicochemical properties and the toxic nature of some NPs contribute to the complexity and inconsistent findings regarding the specific endocytic route involved in the cellular uptake of NPs ([Chou et al., 2011](#)). To minimize such limitations, we used non-cytotoxic and commercially available polystyrene NPs which are suitable for quantitative cellular uptake studies and were previously used as model NPs ([Dos Santos et al., 2011](#)). The aim of the present study was to systematically investigate the cellular uptake mechanisms and to explore the factors affecting cellular uptake of polystyrene NPs. In particular, we wanted to investigate whether a single cell type employs several uptake mechanisms simultaneously to internalize a given type of NPs.

## Materials and methods

### Polystyrene latex beads and molecular probes

Fluorescent polystyrene latex beads of different sizes (20 nm, 100 nm, 200 nm, 500 nm, 1  $\mu$ m and 2  $\mu$ m) were purchased from Life Technologies (F-8888, Darmstadt, Germany) at 2% solids and used without any further modification. The beads were sonicated (Bandelin Sonorex Super RK 106, Berlin, Germany) for 10 min immediately prior to every experiment and were used at a 1:1000 v/v dilution from the 2% solids stock for all experiments unless it was mentioned. FM4-64FX dye (F34653) which is a fixable analog of FM 4-64, Hoechst 33342 (H3570) and LysoSensor Blue DND-167 (L-7533) were similarly purchased from Life Technologies. AlamarBlue cell viability assay reagent was purchased from Trinova Biochem GmbH (Giessen, Germany) and all were used according to the manufacturer's instructions.

### Drug treatment

For inhibition of distinct types of endocytosis pathways, cytochalasin D (C8273), wortmannin (W1628), chlorpromazine hydrochloride (C8138), ikarugamycin (SML0188) and dynasore (D7693) were purchased from Sigma-Aldrich (Deisenhofen, Germany) and dissolved in DMSO to make stock solutions that were further diluted in medium to make their final working concentrations. Oligodeoxynucleotides containing unmethylated cytosine-phosphate-guanine (CpG ODN 1668) with the sequence TCCATGACGTTCTGTATGCT were purchased from Eurofins MWG Operon (Ebersberg, Germany), diluted in distilled water and used at 2.5  $\mu$ g/ml concentrations to activate macrophages.

### Cell culture

Primary bone marrow-derived macrophages (BMDM) were generated from bone marrow of BALB/c mice (Charles River Breeding Laboratories, Sulzfeld, Germany) according to the following protocol. The mouse was sacrificed by cervical dislocation. After disinfecting all external surfaces with 70% ethanol, tibia and femur were surgically removed without damaging the epiphysis and placed into a 50 ml polypropylene tube containing phosphate-buffered saline (PBS). The bone marrows were opened by a sharp scissor in conditioned Dulbecco's Modified Eagle Medium (DMEM) containing 10% fetal calf serum (heat-inactivated), 5% horse serum (heat-inactivated), 50  $\mu$ M  $\beta$ -mercaptoethanol, 10 mM

HEPES buffer, 4 mM L-glutamine, 1% non-essential amino acids and 15% L929 macrophage-colony stimulating factor (M-CSF), and flushed with the medium in a 1 ml syringe (with 26G needle). The stem cells were then centrifuged (300 × g, 10 min, 4 °C) and counted in 1:10 dilution in trypan blue solution using a Neubauer chamber (0.1 mm depth). After incubation for 6 days at 37 °C and 5% CO<sub>2</sub> (20 mm × 100 mm suspension plates; Sarstedt, Nümbrecht, Germany), primary BMDM were harvested by scraping. The L929 fibroblasts from Leibniz DSMZ (German Collection of Microorganisms and Cell Cultures, DSMZ-No ACC-2, Braunschweig, Germany) were cultivated and maintained in complete DMEM containing 50 µM β-mercaptoethanol, 1% non-essential amino acids, 10% fetal calf serum (heat-inactivated), 10 mM HEPES buffer, 200 mM L-glutamine and 1% penicillin-streptomycin solutions. Similarly, the 293T kidney epithelial cells (DSMZ-No ACC-635) were cultivated and maintained in high glucose (4.5 g/l) DMEM without L-glutamine and phenol red but containing 10% fetal calf serum (heat-inactivated), 200 mM L-glutamine and sodium pyruvate. The 293T epithelial cell and L929 fibroblast cell lines were sub-cultured for at least two passages before being used for the experiments. The epithelial cells were trypsinized and fibroblasts were scraped to obtain single cell suspensions. All three cell types were then diluted 1:10 in trypan blue and counted in a Neubauer chamber. The numbers of cells were adjusted to 2 × 10<sup>5</sup> cells per ml for all cell types and the cells were ready to be exposed to NPs in the respective experiments. All the three cell types were treated under equivalent cell culture conditions and exposed to the same NP batch and doses in all the experiments.

#### Flow cytometry

Cells were grown as described above and were harvested, treated with NPs at a 1:1000 v/v dilution from 2% solids stocks for the indicated periods, and then fixed with 4% paraformaldehyde. After washing the fixed cell suspensions twice (300 × g, 10 min, 4 °C), 1 × 10<sup>6</sup> of cell were transferred into fluorescence-activated cell sorter (FACS) tubes and centrifuged (750 × g, 4 °C, 10 min). The cell pellets were resuspended in 1 ml buffer (0.1% sodium azide, 2.5% FCS in PBS) and washed again in 1 ml buffer. The pellet was then finally resuspended in 300 µl of the buffer for measurement. To make sure to get enough material for analysis, 20,000 total events were acquired per sample by using the MACS Quant Analyzer (Miltenyi Biotec, Bergisch Gladbach, Germany) at low rate based on the same instrument setting for all measurements. The data were analyzed using FlowJo software (Tree Star Inc., CA, USA).

#### Macrophage infection by *Leishmania major*

The cloned virulent *Leishmania major* isolate MHOM/IL/81/FE/BNI was maintained by continuous passage in female BALB/c mice. Promastigotes were grown in 96-well blood agar cultures. For the experiments described here, they were collected into a 50 ml tube and washed twice with 20 ml of PBS at 3000 × g, 10 min at room temperature (RT). After suspending the pellet in 2 ml of complete Roswell Park Memorial Institute (RPMI) medium containing 10% fetal calf serum (heat-inactivated), 2 mM L-glutamine, 10 mM HEPES buffer, 0.05 mM β-mercaptoethanol solution, gentamicin (50 µg/ml) and penicillin G (100 U/ml), the promastigotes were counted in 1:20 dilution in PBS using a Neubauer counting chamber (0.02 mm depth). BMDM were used at 2 × 10<sup>5</sup> cells per ml and incubated for 4 h, to enable proper attachment to the bottom of the culture plate, before infection by the parasite. The promastigote number was adjusted to 3 × 10<sup>6</sup> cells per ml to achieve an infection rate of macrophages to promastigotes (cell/parasite ratio) of 1:15. In order to infect BMDM with *L. major*, the supernatant was discarded and an equal volume of complete RPMI medium containing

the promastigotes' suspension was added. After incubating (37 °C, 5% CO<sub>2</sub>) for 12 h, the medium containing the extracellular parasites was removed from the plates and washed three times with the same medium in order remove all extracellular parasites and consequently, avoid any possible competition between the parasite and NPs for cellular uptake. Similarly, non-infected control cells were washed and replaced with equal volume of the new medium. Both non-infected and infected BMDM were then incubated with NPs at 1:1000 v/v dilutions for different time points alone or with 30 min pre-activation by CpG ODN. The medium was replaced with 10 ml ice-cold PBS and incubated on ice for 10 min, scraped with a cell scraper, transferred to 15 ml tubes and washed three times at 300 × g, 4 °C for 10 min, before the accumulations of the NPs were measured by flow cytometry.

#### Transmission electron microscopy

BMDM were incubated with the 100-nm NPs at a 1:1000 v/v dilution at different time points. The cells were then washed and fixed with 1 ml of 2.5% buffered 0.2 M cacodylate in glutaraldehyde at 4 °C overnight. Thereafter, the cells were washed five times (300 × g, 5 min at RT) in 0.5 ml of 50 mM cacodylate buffer (pH 7.2) with incubation at RT for 3 min between each washing step. The cells were again fixed with 0.2 ml of 2% buffered OsO<sub>4</sub> containing 25% H<sub>2</sub>O, 25% 0.2 M cacodylate and 50% OsO<sub>4</sub> at 4 °C overnight. The cells were washed five times in 0.5 ml of H<sub>2</sub>O (1200 × g, RT, 5 min) with three min incubation before each washing step. The cells were further incubated with 0.1 ml of 0.5% aqueous uranyl acetate (Sigma-Aldrich) overnight at 4 °C for contrast. The cells were similarly washed five times in 0.5 ml of H<sub>2</sub>O. The cells were then dehydrated by washing in 0.5 ml of 50%, 70%, 90%, 96% and 100% ethanol concentrations, respectively, with incubation for 30 min at 4 °C before washing (1200 × g, 4 °C, 5 min) in each ethanol concentration. The cells were again incubated in 0.5 ml of 100% ethanol at RT for 30 min and washed at 1200 × g at RT for 5 min. They were then incubated twice in 0.5 ml ready-made 100% propylene oxide at RT for 30 min and washed once after the first incubation at 1200 × g, RT, for 5 min. Finally, the cells were transferred to tubes, centrifuged and embedded carefully without disturbing the cell sediment with 1:1 ratio of Epon 812 to propylene oxide overnight at RT for dehydration. After removal of the supernatant of Epon and propylene oxide on the next day, the cells were embedded again in pure Epon for 21 h at RT and transferred to 60 °C for 2 days for polymerization. Subsequently, the samples were ultrathin sectioned, mounted on 300-mesh grids, stained with uranyl acetate and lead citrate, analyzed with transmission electron microscopy (TEM) and imaged at an accelerating voltage of 80 kV.

#### Fluorescence and confocal microscopy

The cells were treated with the NPs at a 1:1000 v/v dilution at different time points in culture dishes. The media were removed and replaced with PBS before scraping and harvesting the cells from the culture dishes. The cells were then added to 15-ml tubes for further washing (300 × g, 10 min, 4 °C), fixing with 4% paraformaldehyde and further three times washing with PBS. Finally, 10 µl of solution containing the cells were added to slides and covered with cover slips for microscopic examinations. We used a live video fluorescence and confocal microscopy imaging system (Leitz, Wetzlar, Germany).

#### Cytotoxicity assay

Cytotoxicity against BMDM was assessed for inhibitors and polystyrene NPs using the alamarBlue cell viability assay as previously described (Ponte-Sucré et al., 2009). It is a redox-sensitive

assay that quantitatively measures cell viability and proliferation using fluorescent or colorimetric detection strategies. Briefly, after  $2 \times 10^5$  per ml BMDM were incubated with the inhibitors or polystyrene beads in 96-well plates for 24 h, alamarBlue dye was added to each well at 10% concentration and incubated for further 24 h at 37 °C. The OD values were then measured by ELISA reader.

#### Statistical analysis

Values are given as mean  $\pm$  SE and significant differences were determined by using unpaired Student's t test (GraphPad Prism version 5, San Diego, CA, USA). For quantitative colocalization analysis, ImageJ (freely available software) was used. Normalization and percentage calculations based on mean fluorescence intensity (MFI) of the treated cells as compared to the control were also used in flow cytometry data analyses.

#### Results

##### *Cellular uptake mechanism of NPs based on endosomal markers*

We used fluorescent polystyrene latex beads (NPs) to follow their uptake mechanisms in BMDM. According to the supplier's information, the polystyrene NPs used in this study were prepared through polymerization reaction with styrene that terminates with a carboxyl moiety and their diameters were measured by TEM. They are spherical polystyrene NPs loaded with dyes to create intensely fluorescent signals that show little photo bleaching. The dye used for making all the polystyrene NPs fluorescent was physically absorbed by the polystyrene. We checked whether the dye is stably retained in the polystyrene NPs without leakage by incubating the fluorescent NPs with BMDM at 37 °C at different time points and observation under confocal microscopy. There was no indication for dye leakage and the polystyrene NPs were highly fluorescent with a distinct localization inside the cells (Supplementary Fig. S1A). The free dye distribution throughout the cytoplasm as a result of diffusion across cells seems to be very little. The dye is largely hydrophobic, well dispersed and retained within the hydrophobic

polystyrene matrix when the beads are kept in an aqueous solution and are also widely used as a model for NPs-cell interaction studies. We then assessed the cytotoxicity of the polystyrene NPs toward host cells by using the alamar Blue® cell viability assay. The results showed that the polystyrene NPs were not toxic even at a 10 times higher concentration than the one used in the experiment (1:1000 v/v dilution from the 2% solids stock) (Supplementary Fig. S1B). Next, we investigated the cellular uptake mechanisms of the polystyrene NPs by labeling with endocytosis marker FM4-64FX. The FM4-64FX dye immediately stains the plasma membrane by becoming inserted and anchored in the outer leaflet of the plasma membrane lipid bilayer. Only after internalization, the dye becomes localized to the inner leaflet of endocytic vesicles. The BMDMs were incubated with the NPs and 10  $\mu$ M FM4-64FX for 30 min in phenol-free complete RPMI, harvested and washed three times with PBS before imaging. Under fluorescence microscopy, we observed co-localizations of FM4-64FX with the NPs inside the cells (Fig. 1). We repeated this experiment by confocal microscopy and have also confirmed co-localizations of the NPs with endocytic markers (data not shown). Quantitative colocalization analysis by ImageJ showed that about 95.8% of FM4-64FX colocalizes with the NPs while 97.06% of the NPs overlap with the FM4-64FX (Supplementary Fig. S2B (A)). The co-localizations of the NPs and FM4-64FX dye indicate internalization via a shared mechanism and suggested endocytosis to be responsible for the uptake of the polystyrene NPs. The results obtained by using 20 nm and 100 nm polystyrene NPs were similar.

##### *Effects of energy and time on the mechanisms of NP uptake*

Endocytosis is an energy-dependent cellular process. In order to distinguish whether NP uptake was an active or a passive process, BMDM were generated and treated with 20 nm or 100 nm NPs for different time points either at the physiological temperature of 37 °C or at 4 °C. After fixation with 4% paraformaldehyde and three times washing with PBS, the NP uptake was quantified by flow cytometry and 20,000 total events were acquired. The percentages of uptake were then calculated based on relative MFI of cells kept at 4 °C versus cells kept at 37 °C for each time point. For

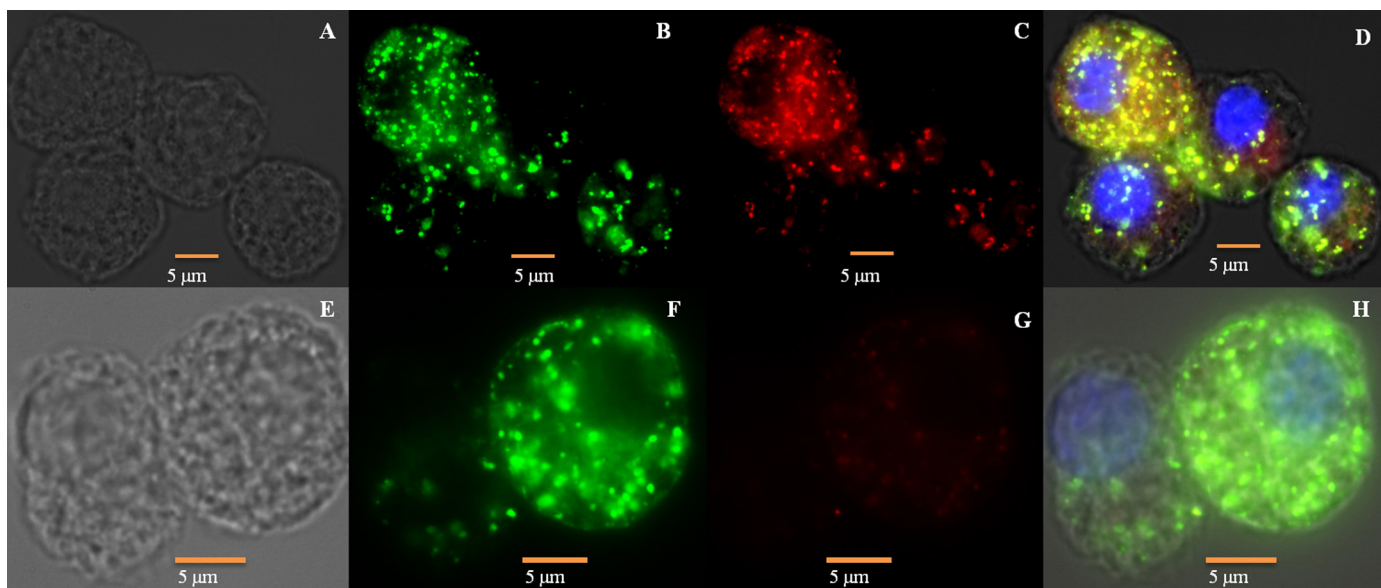


**Fig. 1.** Fluorescence microscopy images of BMDMs after 30 min of incubation with 20 nm (A–D) NPs showing co-localization with the endosomal marker FM4-64FX. Images (E–H) are negative control cells treated with only the NPs. Bright field (A and E), the NPs (B and F), endosomal marker FM4-64FX (C and G), and merge of the channels (D and H) are depicted. Hoechst 33342 was used to stain the nucleus and the images are representatives of two independent experiments. Cells treated with only FM4-64FX and untreated cells for negative control experiments are shown in supplementary Fig. S2A.

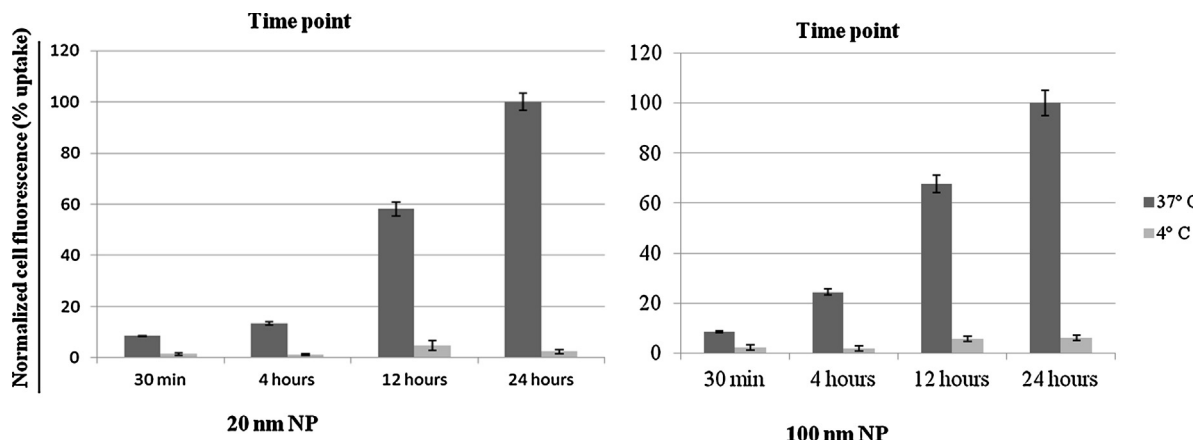


**Fig. 2.** Flow cytometric analyses of the effects of temperature and time on the uptake of 20 nm and 100 nm polystyrene NPs by BMDMs. Cells were pre-incubated on ice for 10 min before exposure to NPs followed by incubation at 4°C for further 30 min, 4 h, 12 h or 24 h while the control groups of cells were incubated at 37°C for the respective time points throughout the incubation period. Normalized MFI values of three to six independent experiments are shown and the values are given as mean  $\pm$  SE.

normalization purposes and improvement of clarity, the MFI values of cells kept with the NPs at 37°C for 24 h were set as 100% and then compared with the other cells kept at both temperatures. The results of the flow cytometric analyses showed a time-dependent cellular uptake of the NPs under equivalent cell culture conditions (Fig. 2). With increasing time of exposure to the NPs, the normalized MFI of the cells were increasing from 8.48% at 30 min to 100% at 24 h showing a time-dependent intracellular accumulation. Similarly, fluorescence microscopy and TEM studies clearly confirmed time-dependent accumulations of the NPs inside the cells (Figs. 3 and 4). However, incubating the BMDM with the same NPs at 4°C under equivalent cell culture conditions resulted in a strong reduction of the uptake at all considered time points, indicating only limited uptake at low energy (Figs. 2 and 5). As there is no exocytosis expected at 4°C we conclude that the limited accumulation of NPs in cells were as a result of reduced uptake. Thus, the NP uptake is an active process and strongly temperature- and time-dependent. Moreover, regardless of the incubation period, we observed similarly low intracellular fluorescence (about 5%) among cells kept at 4°C (Fig. 2). Likewise, fluorescence microscopy images show similar limited uptake at 4°C at all time points (Fig. 5). The uptake study results for both 20 nm and 100 nm NP sizes were similar (Fig. 2).

#### Effect of cell types on uptake mechanisms

The uptake mechanisms and pathways of NPs in different cells are not fully known. To investigate the uptake potentials of BMDM, L929 mouse fibroblasts and 293T human embryonic kidney epithelial cells, each cell type was cultured and treated with NPs under equivalent cell culture conditions. Regardless of the differences in their biological properties, such as size and doubling times, all the cell types were treated with the same NP batch and doses. The uptake potential of each cell type was then quantified by flow cytometry. The results of flow cytometric analyses showed that after 24 h of incubation, BMDM had taken up 100 or 5.5 times more NPs than 293T epithelial cells or L929 fibroblasts, respectively (Fig. 6). Similar results were observed using fluorescence microscopy for each cell type (data not shown), suggesting that the capacity to take up NPs differs significantly among different cell types. Moreover, the uptake rate of NPs was measured at different time points in each cell type in order to investigate their uptake kinetics. The results revealed that BMDM take up 33.8, 60.9 or 64 times higher numbers of NPs than 293T epithelial cells at 30 min, 2 h

or 4 h incubation periods, respectively (Fig. 6). Compared to L929 fibroblasts, BMDM take up 1.9, 4.7 or 5 times more NPs at 30 min, 2 h and 4 h, respectively (Fig. 6). Even though the kinetics of the uptake varies between the cell types throughout the incubation period, the relative uptake differences were significant at all considered time points.

#### Effect of particles' sizes on uptake mechanisms

We further explored the effect of particles' sizes on dictating uptake of NPs into the three cell types by considering additional sizes of polystyrene NPs (200 nm, 500 nm, 1  $\mu$ m and 2  $\mu$ m). BMDM, L929 and 293T cells were cultured and treated with the various sizes of NPs under equivalent cell culture conditions. The uptake potential of the three cell types at different time points were then quantified by flow cytometry. Normalization was done based on the MFI of the cells after incubation with the NPs. The cell type which has highest MFI at 18 h was set as 100% for each NPs size for normalization to facilitate easy comparisons. The results showed that the MFI of the NPs increases according to their size in all the three cell types. Unexpectedly, flow cytometry results showed that the relative uptake efficiency of 293T and L929 are much higher for larger size NPs than smaller size as compared to BMDM (Fig. 7 and Supplementary Fig. S6). To confirm this observation, we conducted confocal microscopy study to see the relative uptake of different sizes of NPs (200 nm, 1  $\mu$ m and 2  $\mu$ m) by the three cell types and the results clearly supported this idea (Supplementary Fig. S7). Conversely, the smaller the particle size, the higher the relative uptake potential of BMDM as compared to L929 and 293T cells. Moreover, regardless of the particles' sizes, longer incubation period were accompanied by the higher uptake (MFI) in all the three cells types. In general, it showed that the internalization extent and kinetics of NPs uptake varies based on particles' sizes and cell types.

#### Infection with *L. major* impairs the potential of macrophages to take up NPs

*L. major* is an obligate intracellular protozoan parasite that causes infection in host macrophages. It is the causative agent of cutaneous leishmaniasis. *Leishmania* parasites have developed sophisticated strategies to manipulate the host macrophage responses to establish successful infection and ensure their own survival by triggering several pathways (Dogra et al., 2007; Gregory et al., 2008). Particularly, it has been shown that macrophage endocytosis capacity is controlled by stimulatory and inhibitory

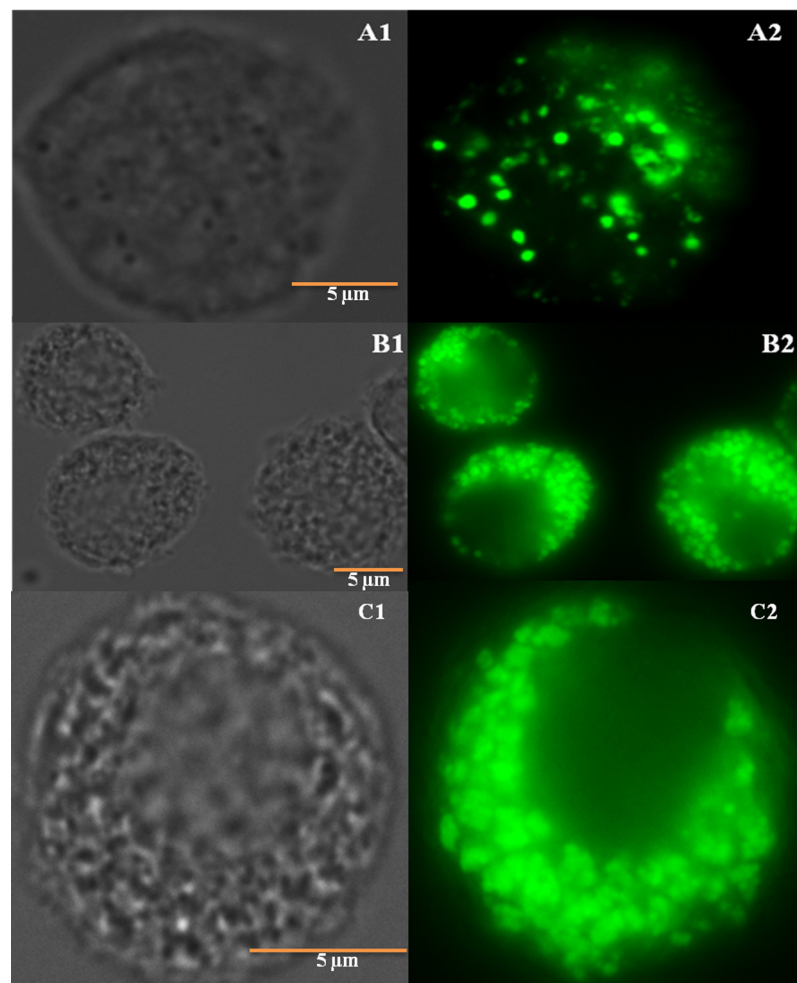


**Fig. 3.** Fluorescence microscopy pictures showing time-dependent accumulations of 100 nm polystyrene NPs in BMDMs. Time-dependent differences in relative accumulation of the NPs after incubation with BMDM for 30 min (A1, A2), 6 h (B1, B2) and 12 h (C1, C2) can be observed. The green channel A2, B2 or C2 shows the polystyrene NPs while A1, B1 or C1 represents the bright field. The pictures are representatives of two independent experiments.

mechanisms (Park et al., 2013). For instance, some intracellular pathogens impair innate immunity through impairment of macrophage endocytosis mechanisms. Moreover, stimulatory molecules like CpG ODN have been shown to enhance the phagocytic activity of macrophages. We therefore hypothesized that infection of macrophages by *L. major* may negatively influence their NP uptake potential and consequently affect the application of NPs in drug delivery systems against leishmaniasis. To test this hypothesis, BMDMs were generated, infected with *L. major* for 12 h and exposed to NPs for different time points at 37 °C. We then measured the cellular uptake potential of the infected BMDMs compared to non-infected macrophages by flow cytometry. The results show that the uptakes of NPs by BMDMs were decreased by at least 1.83 times (from 64% to 35%) when infected with *L. major* (Fig. 8) at 24 h. At all considered time points, infection of BMDMs with *L. major* resulted in significant decreases of the NP internalization potential indicating that the parasite has an inhibitory effect on the ability of macrophages to take up NPs (Fig. 8 and Supplementary Fig. S3). Furthermore, we explored whether activation of *L. major*-infected macrophages by CpG ODN may rescue the decrease in the uptake potential of infected macrophages. The infected and non-infected BMDMs were incubated with the same doses and batch of NPs for 24 h alone or with 30 min pre-activation by CpG ODN. The flow cytometry data showed that the NP-uptake potential of *L. major*-infected BMDM could be restored by activating them with CpG ODN (Fig. 8).

#### *Ultrastructural analyses of membrane morphology reveal multiple cellular uptake mechanisms*

TEM studies were conducted to further confirm endocytosis as uptake mechanism of the NPs and to investigate the specific routes underlying endocytosis in BMDMs. As BMDMs take up extracellular material by a wide range of mechanisms, they allowed us to study the cellular uptake of NPs via a variety of possible entry routes. The data showed that the NPs are accumulated in membrane-bound intracellular vesicles as early as 30 min in BMDM, confirming the involvement of endocytosis in NP uptake (Fig. 9 indicated by EN). Furthermore, ultrastructural plasma membrane invaginations and protrusions documented the involvement of endocytosis (Fig. 9A-E). A few particles seem to be localized in the cytoplasm freely and are not membrane-bound. However, the harsh TEM sample preparation processes may affect the membrane surrounding polystyrene NPs and make them fragile. Furthermore, due to the level/position of the cell sectioning, it may also be difficult to see the membranes surrounding some NPs. Thus, the observation of free NPs in the cytoplasm may not necessarily suggest the involvement of non-endocytic uptake mechanisms.

By closely looking at the ultrastructural morphology of nascent endocytic intermediates, we observed different numbers of NPs partially surrounded by plasma membranes invaginations or protrusions of distinct ultrastructures. These distinct structures do not seem to be simple NPs attachment to surface of the cell membrane

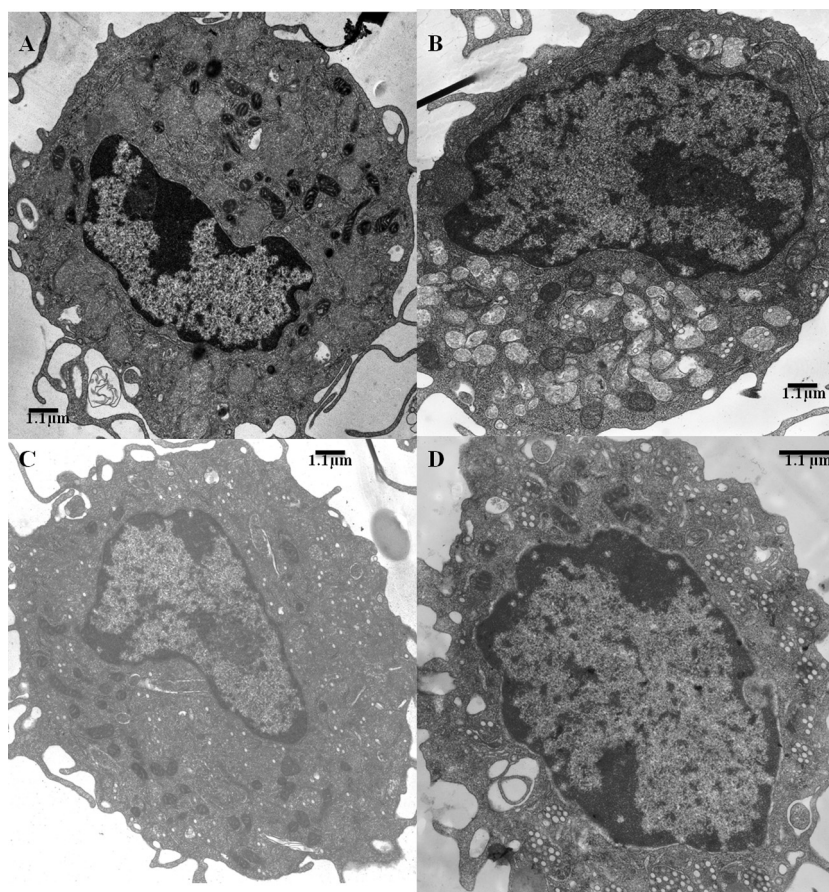


**Fig. 4.** TEM pictures showing accumulations of 100 nm polystyrene NPs in BMDMs in time-dependent manner. In these pictures, A represents randomly selected BMDM as negative control whereas picture B, C or D shows relative accumulation of the NPs at 30 min, 6 h or 12 h incubation time, respectively. The white particle structures are the polystyrene NPs.

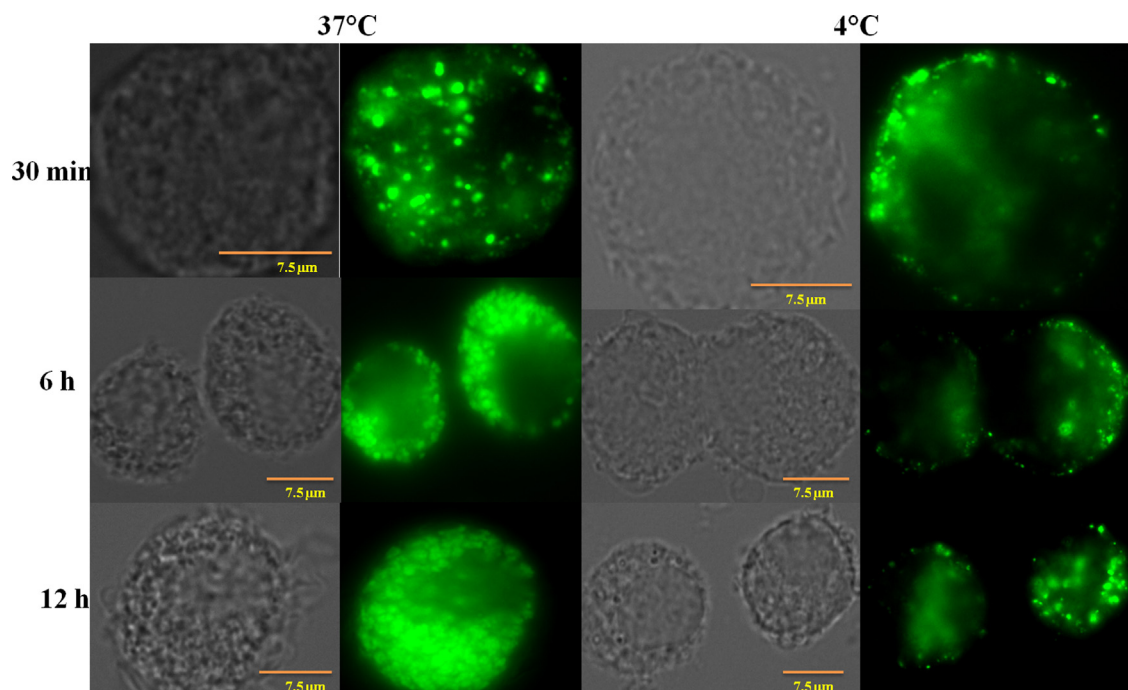


**Fig. 5.** Fluorescence microscopy images showing the effect of temperature and time on the uptake of 20 nm polystyrene NPs by BMDMs. The relative uptake of NPs increased in a time dependent manner at 37 °C while it was strongly reduced at 4 °C. For cells incubated at 4 °C, the time difference seemed to have no effect. Bright field and the NPs (green) for each temperature and time point are depicted. The pictures are representatives of three independent experiments.

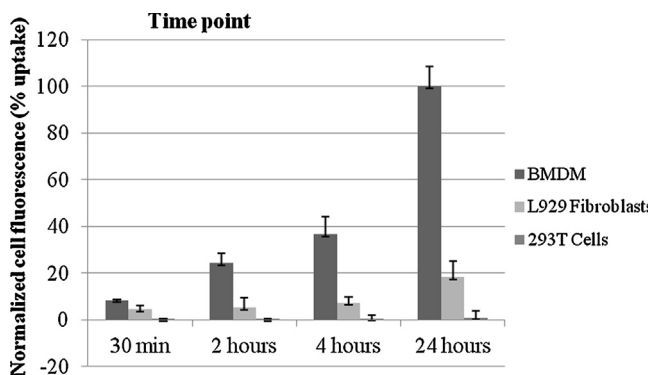


**Fig. 6.** Relative uptake levels of 20 nm polystyrene NPs by different cell types (BMDMs, L929 fibroblasts or 293T epithelial cells) at different time points. At all considered time points, the flow cytometric analyses showed clear differences in the relative uptake of NPs by the three cell types, being highest in macrophages and lowest in epithelial cells for 20 nm sizes. The results are from three independent experiments and the values are presented as mean values  $\pm$  SE. Normalization was done based on MFI from flow cytometry data. The detail representative flow cytometric data including dot plot, histogram and MFI for both treated and untreated negative cell at different time points are shown in Supplementary Fig. S5.

because we could not observe such distinct structures (NPs containing cell membrane structures) throughout the cell membrane surface. Indeed, the coat structures of the membrane surface closer to the NPs are also observable in some routes (Fig. 9). Furthermore, it has been documented that the ultrastructural morphology of membrane invaginations and protrusions provides basic criteria for the identification of different endocytic pathways involved in the internalization processes (Hansen and Nichols, 2009; Kumari et al., 2010; Xu et al., 2013). Based on such plasma membrane morphology, our TEM results showed that NPs are internalized by BMDMs via multiple endocytic routes simultaneously (Fig. 9A–E).

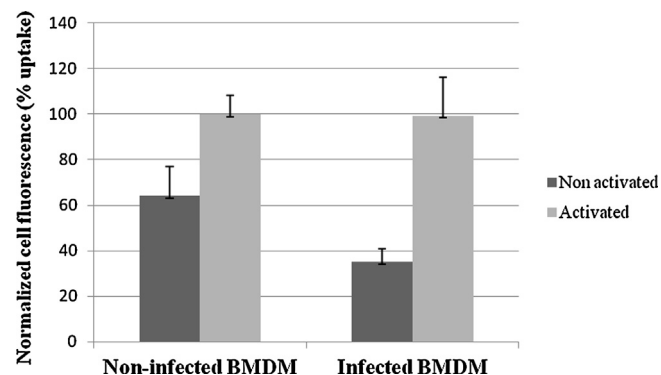


**Fig. 8.** Flow cytometric data showing the effect of *L. major* infection and cell activation status on cellular uptake of 20 nm NPs by BMDMs. The infection significantly reduces the uptake potential of BMDMs while activation CpG ODN rescues it. Moreover, the uptake potential of infected macrophages was significantly higher than that of non-infected macrophages ( $P=0.002$ ) at 24 h. The values are given as mean  $\pm$  SE from three independent experiments. Normalization was done by setting MFI of infected and CpG activated BMDM as 100% for clarity.

The ultrastructure in Fig. 9B shows the cell surface membrane deformations forming cup-like structures by trying to encircle the particles and suggests early process of phagocytosis. Similarly, the ultrastructure in Fig. 9E shows plasma membrane protrusions or ruffles that collapse onto and fuse with the plasma membrane by trying to generate large endocytic vesicles (unlike phagocytosis, these protrusions do not ‘zipper up’ along the NPs) which is indicative of macropinocytosis. The structure in Fig. 9A shows membrane invaginations forming a more or less homogenous, symmetric polygonal lattice. Such ultrastructures are indicative of early clathrin-dependent endocytosis processes. Similarly, Fig. 9D shows a smooth flask-shaped morphological structure suggesting an early caveolin-dependent endocytosis process. Fig. 9C

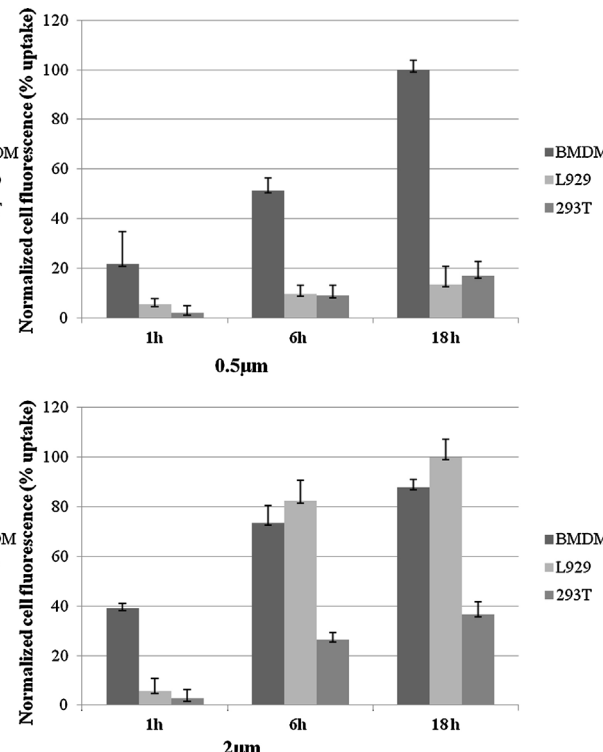
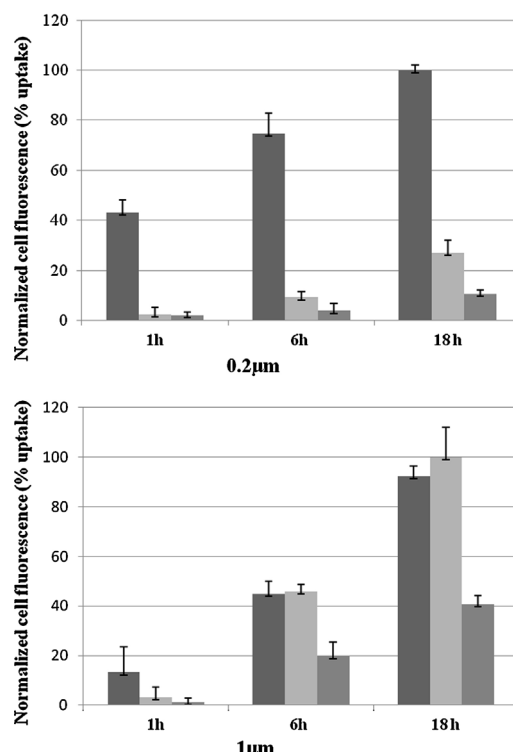


**Fig. 7.** The summary of relative uptake kinetics of 200 nm, 500 nm, 1  $\mu$ m and 2  $\mu$ m polystyrene NPs by 293T epithelial cells, L929 fibroblasts and BMDM at 1 h, 6 h or 18 h incubation times. The data were quantified by flow cytometry and 20,000 events were measured for each samples. The detail representative flow cytometric data including dot plot, histogram and MFI of each experiment are shown in Supplementary Figure S6.

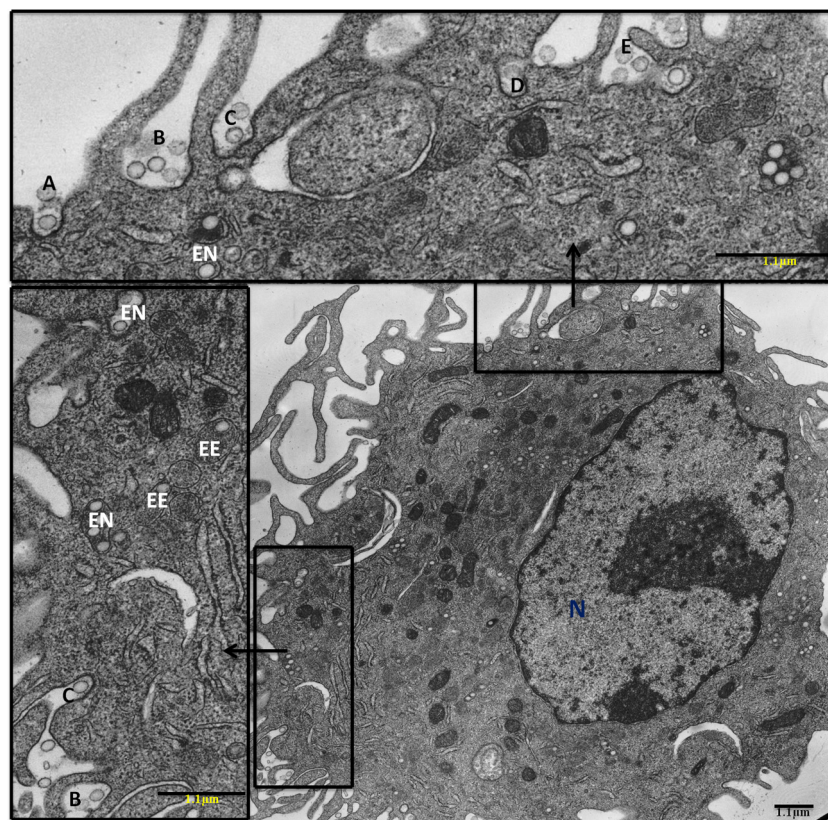


**Fig. 9.** Multiple endocytic pathways used simultaneously by BMDMs to take up 100 nm polystyrene NPs after 30 min of exposure. Based on the ultrastructural morphology of plasma membrane invaginations/protrusions, clathrin-mediated endocytosis (A), phagocytosis (B), clathrin- and caveolae-independent endocytic pathways (C), caveolae-mediated endocytosis. (D), and macropinocytosis (E) are indicated. Intracellular vesicles containing the endocytosed NPs (EN), localization of the NPs in early endosomes (EE) and the nucleus (N) are also shown. Labeled structures (A-E) are the zoomed out portions of the depicted cell for clarity.

demonstrates other clathrin- and caveolin-independent pathways that are characterized by polymorphous or tubulovesicular membrane invaginations in several entry pathways. These ultrastructural analyses showed that 100 nm polystyrene NPs can be internalized by BMDMs in multiple pathways.

#### The ultrastructural morphology of endosomes reveals distinct cellular uptake pathways

The criteria defining specific endocytic pathways are not yet completely identified. However, it has been suggested that the ultrastructural morphology of endosomes containing NPs may reveal the type of endocytosis involved in the uptake of a given type of NPs (Iversen et al., 2011; McMahon and Boucrot, 2011). To further support our observation of multiple uptake pathways based on the ultrastructural morphology of nascent endocytic intermediates at the plasma membrane, the size and morphology of the endosomes containing NPs were analyzed. The result showed that the size and morphology of endosomes containing NPs may be associated with the distinct uptake pathways. The morphology of these endosomes seems to be correlated with the morphology of nascent endocytic intermediates at the plasma membrane. For example, the morphology of endosomes formed by clathrin- and caveolin-independent uptake pathways seem to maintain the tubulovesicular structure of the nascent endocytic intermediates at the plasma membrane (Fig. 10E and F). Similarly, the morphology of endosomes formed by caveolae-dependent endocytosis seems to conserve the well-defined flask shape of nascent endocytic intermediates (Fig. 10D). Larger endosomes (Fig. 10B) are associated with macropinocytosis/phagocytosis rather than other smaller size pathways like caveolae- or clathrin-dependent

endocytosis. Since the larger size endosomes were observed only after 30 min incubation time (Fig. 10B), it is less likely that the larger size endosome are as a result of fusion of endosomes. Furthermore, we also observed endosomes having similar morphology or size but contains different number of NPs (Fig. 10E and F). This may suggest that the morphology and size of the endosomes containing the NPs is not necessarily adopted in accordance to the number of NPs they may contain. It appears that the morphology of each endosome varies not only based on the number of NPs they contained but also the type of uptake routes. This may further suggest that the distinct ultrastructural morphology of nascent endocytic intermediates corresponds to the distinct uptake routes. Thus, the ultrastructural morphology of endocytic vesicles containing NPs may give a clue about the uptake mechanism of NPs. Consequently, it further supports the notion that BMDM use multiple internalization pathways for a given NPs.

#### Analysis of functionally distinct uptake routes by using inhibitors to block different endocytic pathways

To complement the TEM ultrastructural studies of distinct endocytosis pathways involved in the cellular uptake of NPs, pharmacological inhibitors of various endocytic processes were employed. We used drug concentrations described in previous studies (Herd et al., 2013; Moscatelli et al., 2007; Saha et al., 2013; Vercauteren et al., 2010) in order to be sure that the endocytosis inhibitions are due to the pharmacological effect of the inhibitors rather than their toxicity against the host cell. The cytotoxicity of the selected drug concentrations were further tested with BMDMs by using the alamarBlue® cell viability assay (Supplementary Fig. S1A). The safe concentrations of the inhibitors with relatively

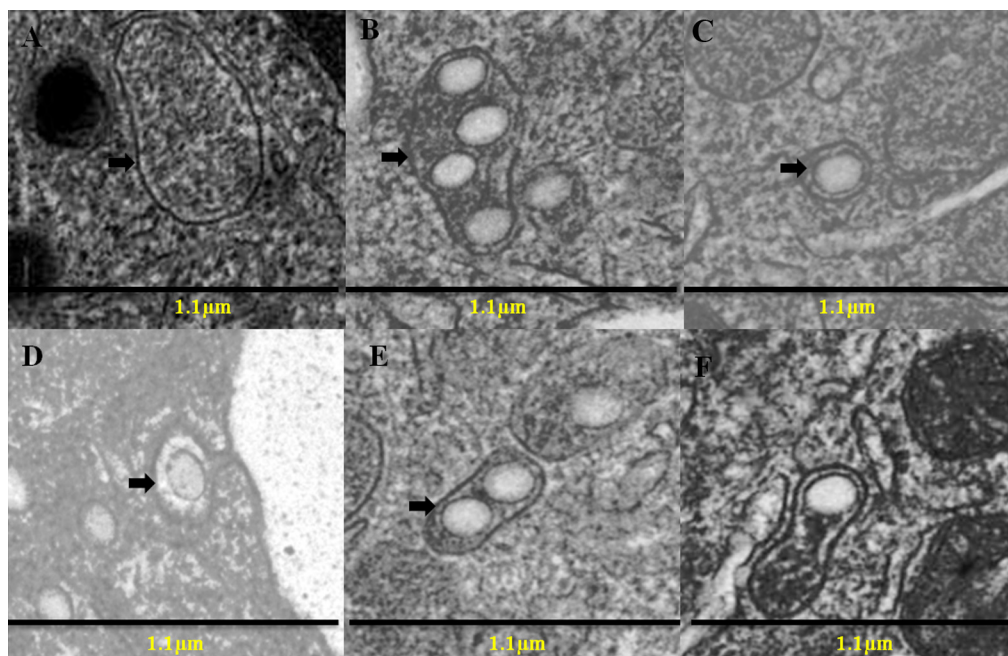


**Fig. 10.** Multiple uptake pathways based on the respective ultrastructural morphology of endocytic vesicles containing the internalized polystyrene 100 nm NP(s) immediately after their internalization by BMDMs. The cells were fixed for TEM after 30 min of incubation with NPs. The arrows indicate endosomes without NPs from untreated cell for negative control (A), phagosomes or macropinosomes (B), endosomes of clathrin-mediated endocytosis (C), endosomes of caveolae-mediated endocytosis (D) and endosomes of clathrin-and caveolae-independent endocytic pathways (E and F).

high inhibition rates in our system were then used for blocking studies. The inhibitors used include wortmannin (12.85 µg/ml), a potent inhibitor of phosphatidylinositol kinase (PI3 K) involved in different endocytic pathways but commonly used as inhibitor of phagocytosis and macropinocytosis (Fernando et al., 2010; Khalil et al., 2006; McMahon and Boucrot, 2011), cytochalasin D (5 µg/ml) which blocks the actin polymerization that participates in a variety of endocytic processes but is commonly used as inhibitor of phagocytosis and macropinocytosis (Iversen et al., 2011), dynasore (25.8 µg/ml), a cell-permeable small molecule that inhibits dynamin GTPase activity needed for several mechanisms including clathrin-dependent endocytosis (Kirchhausen et al., 2008; Sato et al., 2009), chlorpromazine hydrochloride (10 µg/ml) that inhibits a Rho GTPase which is essential for the formation of clathrin-coated vesicles in clathrin-dependent endocytosis (Iversen et al., 2011; Vercauteren et al., 2010) and ikarugamycin (1 µM), an inhibitor of clathrin coated pit-mediated endocytosis (Moscatelli et al., 2007). The BMDMs, L929 fibroblasts, and 293T epithelial cells were cultured and exposed to 100 nm NPs in the same manner as in the TEM study described above except that the cells were pre-incubated with each of the five inhibitors for 30 min at 37 °C. The uptake was measured by flow cytometry after 3 h of incubation in order to keep a balance between allowing sufficient time for enough NPs to enter the cells, and for the pharmacological inhibitors to reduce endocytosis without inducing a shift of the pathways. It has been reported previously that blocking one uptake pathway can result in activation of other endocytic mechanisms (Roth, 2007). The results were then documented as relative uptake (percentage) based on MFI of inhibitor treated cells compared to untreated control cells by setting the average MFI of control cells as 100% (Fig. 11).

The results show that wortmannin inhibited as much as 93.7%, 70.4% and 55.3% of NP uptake in BMDMs, L929 fibroblasts and 293T kidney epithelial cells, respectively. Even though wortmannin is not as specific as other inhibitors, it showed the involvement of phagocytosis and/or macropinocytosis in the uptake of the NPs by all three cell types. Similarly, blocking actin formation by cytochalasin D reduced the NP uptake by 74.3% in BMDMs, 55% in L929

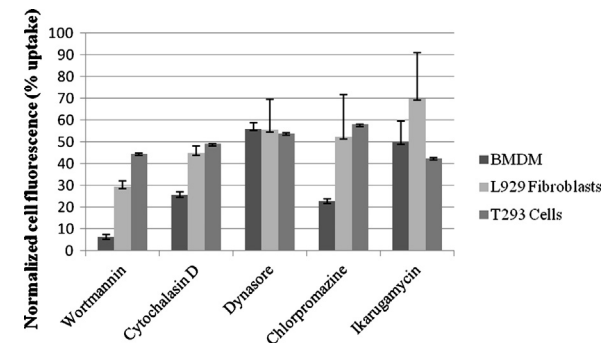


**Fig. 11.** Effects of different pharmacological inhibitors on the uptake of 100 nm polystyrene NPs by different cell types (BMDMs, L929 fibroblasts or 293T epithelial cells) after 3 h of incubation. The MFI values of NPs inside the cells were quantified by flow cytometry in the presence or absence of each inhibitor. The average MFI of control cells without any inhibitor were set as 100% for normalization purpose and easy comparison. Normalized MFI values and standard errors of 3–6 independent experiments are shown. Normalized MFI values and standard errors of 3–6 independent experiments are shown.

fibroblasts and 50.8% in 293T kidney epithelial cells. Blocking actin formation would inhibit macropinocytosis and phagocytosis. However, it has also been reported to participate in several other uptake mechanisms including clathrin-mediated endocytosis and caveolin-mediated endocytosis (Iversen et al., 2011; Nagahama et al., 2011). Therefore, we consider cytochalasin D as nonselective inhibitor of different internalization pathways, but it can point out the existence of macropinocytosis and/or phagocytosis pathways in this scenario again. Chlorpromazine, a drug considered to block clathrin-dependent endocytosis, inhibited the NP uptake by 77.3% in BMDMs while it only inhibited 47.5% and 42% in L929 fibroblasts and 293T kidney epithelial cells, respectively. However, since the Rho-family GTPases are also involved in other pathways – such as phagocytosis and macropinocytosis (Conner and Schmid, 2003) – chlorpromazine cannot be regarded as specific either (Vercauteren et al., 2010). Nevertheless, it may similarly show the involvement of

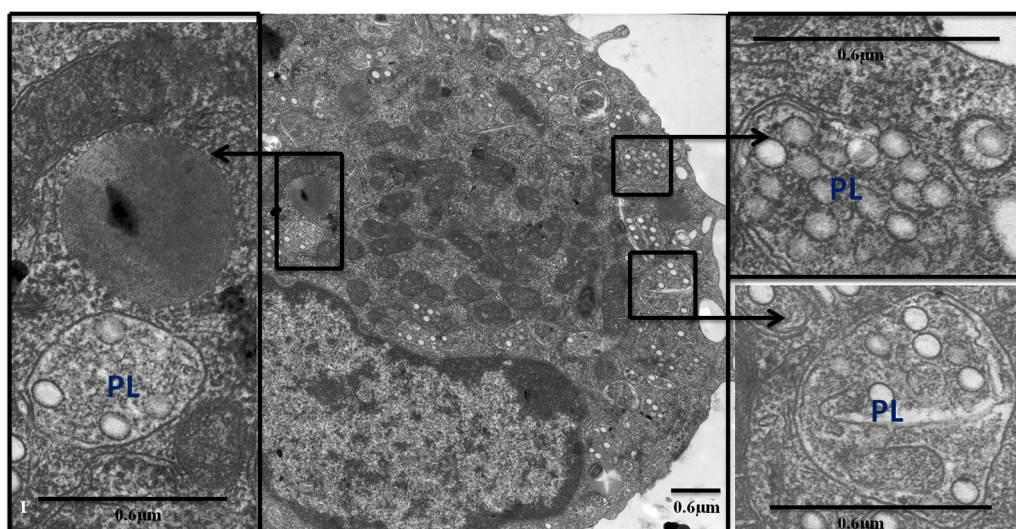


**Fig. 12.** TEM images of randomly selected BMDM showing localizations of the 100 nm polystyrene NPs in late endosomes/lysosomes (PL) after 6 h of incubation. The NPs localizes in the cytoplasm of cell failing to transit through nuclear membrane.

clathrin-dependent endocytosis. Furthermore, using ikarugamycin, the specific inhibitor of clathrin-coated pit-mediated endocytosis resulted in a 50%, 30% and 57.4% inhibition of NP uptake in BMDMs, L929 fibroblasts and 293T kidney epithelial cells, respectively, highlighting the involvement of clathrin-dependent endocytosis in these cell types. Finally, inhibiting dynamin-dependent endocytic pathways including clathrin-dependent endocytosis and caveolin-mediated endocytosis by dynasore reduced the NP uptake by similar rates in all the three cell types (44%, 44.5% and 45% in BMDM, L929 fibroblasts and 293T kidney epithelial cells, respectively). It also suggests that the remaining 55–56% of the NP uptake were via dynamin-independent pathways indicating that all the three cell types can use both dynamin-dependent and dynamin-independent endocytic pathways for the uptake of the NPs. Even though it has been shown that the specificity of pharmacological inhibitors is not sufficient to clearly distinguish endocytic pathways (Vercauteren et al., 2010), the findings support the TEM results regarding the existence and utilization of several distinct endocytic pathways by the three cell types for internalization of NPs.

We used Alexa 448-labeled transferrin (2.5 μg/ml) as positive control for clathrin-dependent endocytosis. As expected, the result show that chlorpromazine efficiently blocked the uptake of transferrin in all the three cell types, and cytochalasin D affected the uptake of the transferrin in BMDMs while other inhibitor even increased the uptake of transferrin. The results are shown in Supplementary Fig. S4.

#### Intracellular trafficking of NPs and their localization in BMDMs

It was then important to analyze the NP trafficking inside BMDMs. The robust endocytic marker FM4-64FX (Fig. 1) and the TEM results (Figs. 9 and 10) confirmed that the NPs were localized in endocytic vesicles (endosomes) immediately after their internalization. NPs were localized in ultrastructural vesicles suggestive of early endosomes as early as 30 min (Fig. 9 indicated by EE) and it seems that only few NPs are transported to early endosomes at this time of incubation. To further follow their trafficking inside BMDMs and study whether internalized NPs are further transited through the endolysosomal pathway, we incubated the cells with NPs for 6 h and performed TEM analysis. As can be seen in Fig. 12 (indicated as PL), the results suggest that the final cellular localization of the NPs is in structures suggestive of late endosomes/lysosomes. The NP distribution inside BMDMs demonstrate that they are exclusively

localized in the cytoplasm but not in nuclei, indicating the failure to transit across the nuclear envelope (Figs. 9 and 12). The localization of NPs in acidic endosomes/lysosomes was further validated by lysosensor blue. This dye is almost non-fluorescent except when inside acidic compartments and used to measure pH of vesicles inside cells. The concentrations of dyes were kept as low as possible (5 μM) to reduce potential artifacts from overloading; however, we could not detect the basal level of acidic vesicles with such concentration of the dye. The results showed that lysosensor blue co-localized with NPs after 6 h of incubation, confirming their localization in acidic pH (Fig. 13). The pKa of lysosensor blue is ~5.1. Thus, we conclude that the NPs are localized in acidic intracellular vesicles during their trafficking in the endolysosomal cascade inside BMDMs. Even though the mechanisms by which internalized particles can escape from endolysosome degradation are complex and not yet fully understood (Yan et al., 2012), their pH level was found to be in the acidic range. As a result, the changes in pH may be also considered as a trigger to activate controlled drug release inside the cytoplasm.

#### Discussion

The use of nanotechnology in every field of science is spreading rapidly and particularly in medicine. Its application improves diagnosis and therapy of diseases through effective delivery of drugs, biopharmaceutical molecules or imaging agents to target cells at disease sites (Kim et al., 2010; Sahay et al., 2010; Smith et al., 2013). For such applications, initial recognition of nanomaterials by the immune system is an essential determinant for the fate and distribution of materials inside the body (Underhill and Goodridge, 2012). Thus, a better understanding of how cells take up NPs may lead to the development of enhanced antigen-, drug- or other molecules-delivery tools. In this scenario, we tried to elucidate the internalization mechanisms of commercially available polystyrene NPs by different mammalian host cells and to explore the factors affecting their uptake. Our results show that as many as 95% of NPs are generally taken up via an energy-dependent process at all considered time points in BMDMs. Although lowering the culture temperature also affects the diffusion of NPs or a passive mode of entry, it has been demonstrated previously that diffusion is not the rate-limiting step for NP uptake into cells and blocking uptake pathways by drugs is a consequence of inhibition of active transport, rather than a consequence of reduced NP diffusion

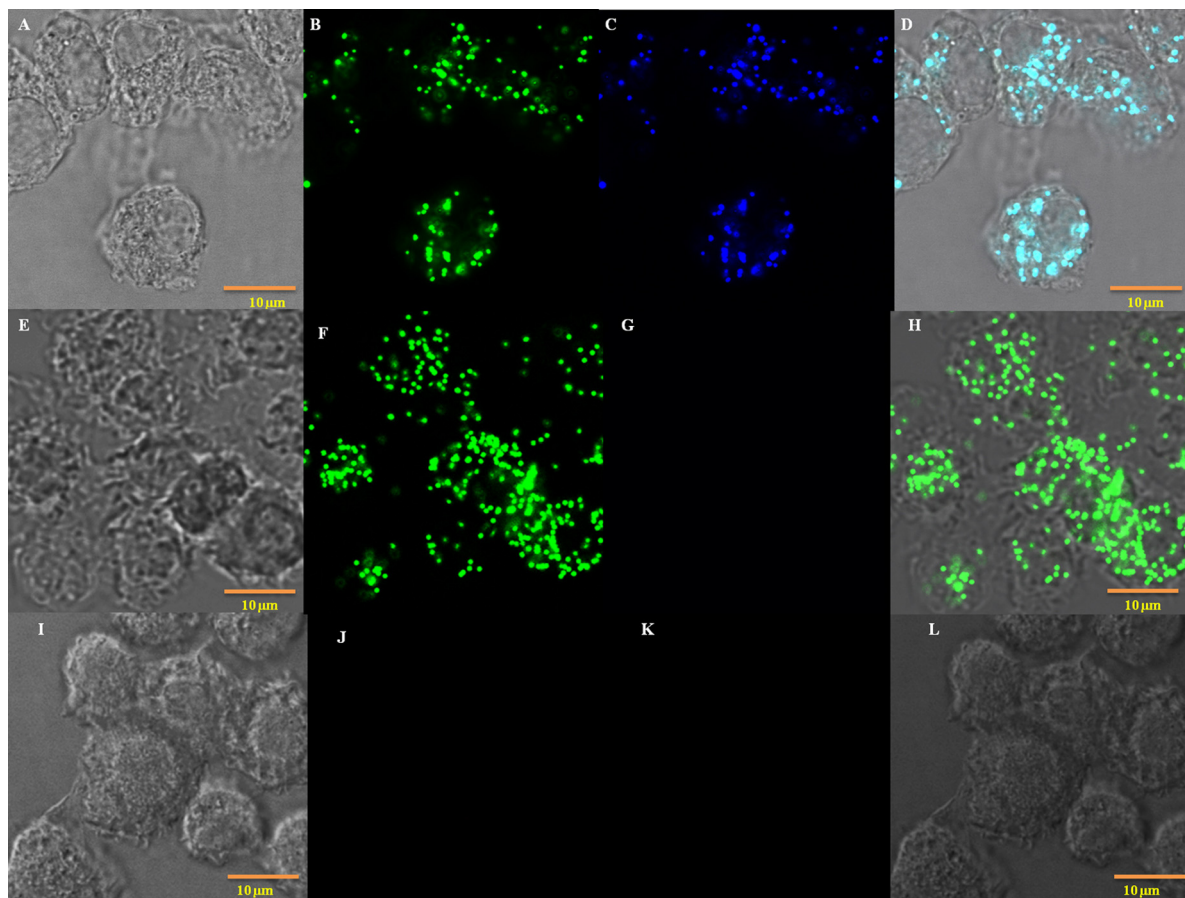


**Fig. 13.** Confocal microscopy images of BMDMs showing the colocalizations of 100 nm polystyrene NPs at a 1:1000 v/v dilution and lysosensor blue staining intracellular acidic pH vesicles at 6 h of incubation. The images indicate bright field (A), green fluorescent polystyrene NPs (B), lysosensor blue (C), overlay (D) and their respective channels for control cells without lysosensor blue (E–H) and negative control cells (I–L). The depicted pictures are representatives of two independent experiments.

([Salvati et al., 2011](#)). This finding is in accordance with other group results showing that cellular uptake of NPs is predominantly mediated by endocytosis ([Albanese et al., 2012; Iversen et al., 2011](#)). In contrast, it has also been reported that NPs are taken up via non-endocytic pathways: for instance, [Mu et al. \(2012\)](#) suggested a passive mode of entry after observing NPs inside cells after exposure at 4 °C for 30 min. We also observed about 5% uptake in cells kept at 4 °C at different time points. However, the status of the cells before exposure to NPs may have some influence on such uptake at 4 °C. Because the cells could have limited energy from pre-incubation at 37 °C that may be exhaustively used for such active cellular processes during the early period of incubation. Indeed, we observed a decrease in uptake at 4 °C when we increased the pre-incubation on ice from 10 min to 30 min before exposing the cells to the NPs (data not shown). Altogether; we conclude that NP uptake seems to be predominantly achieved by endocytic processes in an energy- and time-dependent manner.

The cellular uptake mechanism of NPs is influenced by multiple factors ([Kim et al., 2012](#)) among which the physicochemical properties of NPs are considered to be the main determinants of the import and subsequent intracellular trafficking of the NPs. Particle size and charge is likely the primary factor that governs endocytic uptake of particles. Our in vitro cellular uptake experimental results indicated that the relative uptake efficiency of 293T and L929 increases with sizes of NPs as compared to the BMDM. In contrast to our finding, many groups have shown that cellular uptake is size-dependent but significantly faster for smaller particles than larger particles in antigen-presenting cells ([Li and Schneider, 2014; Shima et al., 2013](#)). However, the non-professional phagocytes like epithelial

cells take up smaller NPs more efficiently than large particle size ([Hu et al., 2007; Kulkarni and Feng, 2013](#)). Interestingly, in line with our finding, it has also been shown that cells non-specialized for phagocytosis were able to internalize NPs as large as 2 μm ([Dos Santos et al., 2011](#)). Our results suggest that the particle uptake might not follow commonly defined size limits for uptake processes by different cells. The difference of the results may have resulted from the diverse approaches. Many size-dependent uptake studies simply compare the uptake efficiency of differently sized NPs by measuring the percentage of uptake by a particular cell without first considering the differences in fluorescence intensity among the different NP sizes themselves. However, we compared the relative uptake potential of the three cell types for a particular particle size at a time so as to ensure that the variations in MFI among the cells types resulted from the difference in uptake potentials rather than fluorescence intensity deviations among the different NP sizes.

Moreover, increasing surface charges of NPs (positive or negative) have been shown to increase particle uptake in comparison with uncharged ones ([Kettler et al., 2014](#)). It has been also suggested that NPs with positive surface charge are taken up more efficiently than negatively charged NPs ([Liu et al., 2013](#)). Another important factor is the degree of aggregation and protein corona. The arrival of NPs in the dynamic extracellular environment may change the protein corona, size or aggregation. These changes may consequently affect many aspects of NP-cell interactions including the mode of particle uptake because the biological identity of a NP depends on the composition of the surrounding biological medium ([Albanese et al., 2014](#)). It has also been shown that increasing NP-incubation time may induce NP aggregation and changes in protein

corona composition that subsequently determine cellular uptake mechanisms (Albanese et al., 2014). We further explored cell types as a factor influencing the NPs entry pathways. We showed that the potential to take up NPs is highly different for BMDM, 293T epithelial cells and L929 fibroblasts, being highest for macrophages followed by fibroblasts for 20 nm NPs, indicating variability of uptake kinetics for the same material in different cell types. This finding is in line with a previous report by Dos Santos et al. (2011) showing that the uptake of different sizes of NPs varies in different cell lines, being highest in macrophages and lowest in the HeLa cells. The differences in the uptake rates of BMDMs (professional phagocytes) and non-professional phagocytes (293T epithelial cells and L929 fibroblasts) may be due to differences in the number or type of endocytic pathways involved to internalize the NPs. In contrast to 293T epithelial cells and L929 fibroblasts, BMDMs may use multiple uptake routes simultaneously for relatively smaller particle sizes. Taken together, it shows that cellular uptake of NPs is influenced by several factors associated with either physiochemical properties of the NPs or its surrounding environments.

Furthermore, we looked whether NP import is influenced by microbial infection. We demonstrated that infection of BMDMs with *L. major* significantly decreased the cellular uptake of NPs. The effect of *L. major* infection on macrophages has been investigated by many researchers and demonstrated that the parasite can subvert macrophage responses by regulating different genes including those responsible for endocytosis and cell adhesion (Dogra et al., 2007; Gregory et al., 2008; Lemaire et al., 2013). However, the mechanisms still remain poorly understood. Previously, we showed that the parasite induces downregulation or upregulation of cytokine and chemokine expression profiles as a mechanism of subversion in *in vitro* cell culture (Steigerwald and Moll, 2005). It represses the production of inflammatory cytokines (TNF- $\alpha$ , IL-6, IL-12) that are essential for their survival and multiplication inside macrophages (Olivier et al., 2005; Steigerwald and Moll, 2005). Moreover, it has been shown that some intracellular pathogens have inhibitory mechanisms to suppress macrophage physiological functions. Recently, it has been shown that macrophages infection with HIV-1 virus would result in impairment of its phagocytic function (Jambo et al., 2014). Similarly, Basu et al. have showed a 2-fold decrease in uptake rate of macrophages through a decrease in endocytosis receptors after infection with *Leishmania* parasites; whereas, recovery of receptor activity and uptake potential were observed after elimination of parasites from macrophages (Basu et al., 1991). Thus, it suggests that the decreased uptake of NPs by *L. major*-infected macrophages may be associated with a kind of 'silencing effect' of the intracellular parasite on BMDMs. We also showed that the activation status of macrophages has a significant effect on their uptake potential. The uptake of NPs was significantly enhanced in CpG ODN-activated and/or infected macrophages as compared to non-activated control cells. It shows that CpG ODN could rescue the decrease in NP uptake by BMDMs infected with *L. major*. These results are also in agreement with the previous findings. Gupta et al. showed that CpG ODN have a promising efficacy against *L. major* in *in vivo* rodent experiments through activation of host immune responses and, consequently, could revert the effect of the parasite on macrophages (Gupta et al., 2011). Similarly, it has also been shown that the endocytic activity of macrophages is enhanced in response to CpG ODN (Utaisincharoen et al., 2003; Wang et al., 2009). As a result, the observed effect of CpG ODN could be either through activation of the macrophages to increase the uptake of the NPs or to kill the intracellular parasite.

The distinct endocytic pathways are highly regulated to control all aspects of intercellular communications and have been associated with many factors. However, it has not yet been fully resolved whether a single cell or cell type uses several uptake pathways

simultaneously for given particles. As can be clearly seen by the TEM and inhibitor study results, a cell may utilize multiple endocytic pathways simultaneously to internalize a given type of particles (Figs. 9 and 10). Interestingly, all these distinct uptake routes were observed in a BMDM after treating with 100 nm NP sizes for 30 min, confirming the use of several routes by cells to take up a given type of NPs. As can be seen by TEM analysis (Fig. 9B and E), an uptake pathway that requires a larger size of NPs (phagocytosis or macropinocytosis) may be triggered by a number of smaller particles, or their aggregates, approaching a specific area of the plasma membrane giving the uptake signal. This signal most probably controls the type of protein recruitment in the area of initiation and the type of endocytic pathway that should be in place for the uptake of NPs via protein-lipid and protein-protein interactions (Le Roy and Wrana, 2005; McMahon and Boucrot, 2011; Olsson, 1995; Sandvig et al., 2011). The sonication steps of NPs to generate single particles are very important in such type of studies since the uptake mechanisms for a specific NP and its aggregate may differ. Even though it is believed that there are several endocytic pathways for uptake of various NPs by a given cell, to our knowledge this is the first evidence based on ultrastructural analysis documenting multiple uptake routes simultaneously to internalize a given type of NPs. Blocking distinct endocytosis pathways by inhibitors corroborated this conclusion. None of the treatments with different inhibitors fully inhibited NP uptake but some inhibited more strongly in one cell type than others (Fig. 11). For instance, wortmannin, cytochalasin D and chlorpromazine inhibited the NP uptake in BMDMs more strongly than in L929 mouse fibroblasts and 293T human embryonic kidney epithelial cells, suggesting some pathway might be more sensitive to the inhibitors in one cell type than the others. In line with our results, a recent study showed that polyelectrolyte multilayer capsules of a few micrometer size are taken up by cells via multiple pathways including lipid rafts, macropinocytosis or phagocytosis (Kastl et al., 2013). The authors used larger particle sizes and, consequently, identified larger size uptake pathways: macropinocytosis and phagocytosis. However, unlike in our study, they could not identify the smaller size uptake pathways like clathrin, caveolin or clathrin- and caveolin-independent uptake pathways. This difference can be explained by the fact that the sizes of the NPs used in this particular experiment were 20 nm or 100 nm, while the sizes of the multilayer capsules were in the micrometer range.

TEM and co-localization studies further showed that the NPs localize in membrane-bound endosomal vesicles soon after their internalizations and are subsequently trafficked to late endosomes/lysosomes. Different from this finding, Johnston et al. (2010) reported that polystyrene NPs are not contained in early endosomes or lysosomes in hepatocytes. On the other hand, many investigators described the particles to enter a lysosome-associated membrane protein 1 (LAMP-1)-positive lysosomal compartment in macrophages (Fernando et al., 2010; Xia et al., 2008). These differences may be explained by the use of different cell types or methodology approaches. Generally, it has been shown that cells internalize NPs by different types of endocytosis, resulting in their accumulation in different endocytic vesicles or tubules after engulfing. They are then transported to early endosomes and either transported back to the membrane surface by exocytosis (not very common in NPs), or further transported through late endosomes or multivesicular bodies to lysosomes for attempting to degrade (Al-Rawi et al., 2011; Iversen et al., 2011; Kang et al., 2008).

## Conclusions

The results presented in this study provide a detailed analysis of multiple cellular uptake mechanisms of fluorescent polystyrene

NPs and factors affecting their uptake mainly in BMDMs. The data show that NPs are rapidly internalized and accumulate in endosomal compartments, indicating their ability to entry into different cells types. Once the NPs are internalized by host cells, they localize in endosomes and then traverse to acidic pH vesicles through the endolysosomal pathways. The NPs uptake is an energy-dependent process that highly depends on NPs' sizes, cell types and time. Cells may use several distinct types of endocytosis pathways simultaneously for the uptake of a given type of particles. Even though particles of larger size (a few micrometers) are usually taken up by phagocytosis or micropinocytosis, our findings suggest that smaller NPs are internalized by multiple endocytosis routes including macropinocytosis, phagocytosis, clathrin-mediated endocytosis, caveolae-mediated endocytosis, and clathrin- and caveolae-independent pathways. The results highlight the complexity of cell-nanoparticle interactions beyond the previous assumptions, and the need of case-by-case studies to achieve the goal of manipulating NPs to control their entry pathways. Furthermore, physicochemical properties of the NPs have been considered as the main factors determining the cellular uptake and intracellular pathways of NPs. However, our study shows that the type of infection or disease pathogenesis and/or the cell activation status also significantly affects the potential of BMDMs to take up NPs. Since this may consequently determine the application of NPs in biomedical delivery systems, our findings emphasize the need to understand the diseases' pathogenesis in order to establish effective and rationally designed drug delivery systems. These observations may enhance our understanding of the application of nanotechnology in biomedical sciences.

## Acknowledgments

R.F. was supported by a fellowship of the German Excellence Initiative to the Graduate School of Life Sciences, University of Würzburg, Germany. The authors are grateful to Prof. Dr. Anke Krueger and Thilo Waag, Institute for Organic Chemistry, and Dr. Uta Schurigt, Institute for Molecular Infection Biology, University of Würzburg, for valuable discussions. We would like to thank Prof. Dr. Richard Lucius, Molecular Parasitology, Humboldt University, Berlin, for his scientific support. We thank the group of Prof. Dr. Georg Krohne, Biocenter of the University of Würzburg, Core Unit for Electron Microscopy, especially Daniela Bunsen and Claudia Gehrig, for help in TEM sample preparation and imaging. We also thank Bianca Röger, Martina Schultheis and Elena Katzowitsch, Institute for Molecular Infection Biology, University of Würzburg, for technical assistance.

## Appendix A. Supplementary data

Supplementary material related to this article can be found, in the online version, at <http://dx.doi.org/10.1016/j.ejcb.2014.08.001>.

## References

- Albanese, A., Tang, P.S., Chan, W.C.W., 2012. The effect of nanoparticle size, shape, and surface chemistry on biological systems. *Annu. Rev. Biomed. Eng.* 14, 1–16, <http://dx.doi.org/10.1146/annurev-bioeng-071811-150124>.
- Albanese, A., Walkley, C.D., Olsen, J.B., Guo, H., Emili, A., Chan, W.C.W., 2014. Secreted biomolecules alter the biological identity and cellular interactions of nanoparticles. *ACS Nano* 8, 5515–5526, <http://dx.doi.org/10.1021/nn4061012>.
- Al-Rawi, M., Diabaté, S., Weiss, C., 2011. Uptake and intracellular localization of sub-micron and nano-sized SiO<sub>2</sub> particles in HeLa cells. *Arch. Toxicol.* 85, 813–826, <http://dx.doi.org/10.1007/s00204-010-0642-5>.
- Basu, N., Sett, R., Das, P.K., 1991. Down-regulation of mannose receptors on macrophages after infection with *Leishmania donovani*. *Biochem. J.* 277, 451–456.
- Briones, E., Colino, C.I., Lanao, J.M., 2008. Delivery systems to increase the selectivity of antibiotics in phagocytic cells. *J. Control. Release* 125, 210–227, <http://dx.doi.org/10.1016/j.jconrel.2007.10.027>.
- Chou, L.Y.T., Ming, K., Chan, W.C.W., 2011. Strategies for the intracellular delivery of nanoparticles. *Chem. Soc. Rev.* 40, 233–245, <http://dx.doi.org/10.1039/c0cs00003e>.
- Conner, S.D., Schmid, S.L., 2003. Regulated portals of entry into the cell. *Nature* 422, 37–44, <http://dx.doi.org/10.1038/nature01451>.
- Couvreur, P., 2013. Nanoparticles in drug delivery: past, present and future. *Adv. Drug Deliv. Rev.* 65, 21–23, <http://dx.doi.org/10.1016/j.addr.2012.04.010>.
- Dogra, N., Warburton, C., McMaster, W.R., 2007. *Leishmania major* abrogates gamma interferon-induced gene expression in human macrophages from a global perspective. *Infect. Immun.* 75, 3506–3515, <http://dx.doi.org/10.1128/IAI.00277-07>.
- Dos Santos, T., Varela, J., Lynch, I., Salvati, A., Dawson, K.A., 2011. Quantitative assessment of the comparative nanoparticle-uptake efficiency of a range of cell lines. *Small* 7, 3341–3349, <http://dx.doi.org/10.1002/smll.201101076>.
- Fernando, L.P., Kandel, P.K., Yu, J., McNeill, J., Ackroyd, P.C., Christensen, K.A., 2010. Mechanism of cellular uptake of highly fluorescent conjugated polymer nanoparticles. *Biomacromolecules* 11, 2675–2682, <http://dx.doi.org/10.1021/bm1007103>.
- Gregory, D.J., Sladek, R., Olivier, M., Matlashewski, G., 2008. Comparison of the effects of *Leishmania major* or *Leishmania donovani* infection on macrophage gene expression. *Infect. Immun.* 76, 1186–1192, <http://dx.doi.org/10.1128/IAI.01320-07>.
- Gupta, S., Sane, S.A., Shakya, N., Vishwakarma, P., Haq, W., 2011. CpG oligodeoxynucleotide 2006 and miltefosine, a potential combination for treatment of experimental visceral leishmaniasis. *Antimicrob. Agents Chemother.* 55, 3461–3464, <http://dx.doi.org/10.1128/AAC.00137-11>.
- Hansen, C.G., Nichols, B.J., 2009. Molecular mechanisms of clathrin-independent endocytosis. *J. Cell Sci.* 122, 1713–1721, <http://dx.doi.org/10.1242/jcs.033951>.
- Herd, H., Daum, N., Jones, A.T., Huwer, H., Ghandehari, H., Lehr, C.-M., 2013. Nanoparticle geometry and surface orientation influence mode of cellular uptake. *ACS Nano* 7, 1961–1973, <http://dx.doi.org/10.1021/nn304439f>.
- Hu, Y., Xie, J., Tong, Y.W., Wang, C.-H., 2007. Effect of PEG conformation and particle size on the cellular uptake efficiency of nanoparticles with the HepG2 cells. *J. Control. Release* 118, 7–17, <http://dx.doi.org/10.1016/j.jconrel.2006.11.028>.
- Iversen, T.-G., Skotland, T., Sandvig, K., 2011. Endocytosis and intracellular transport of nanoparticles: present knowledge and need for future studies. *Nano Today* 6, 176–185, <http://dx.doi.org/10.1016/j.nantod.2011.02.003>.
- Jambo, K.C., Banda, D.H., Kankwatiira, A.M., Sukumar, N., Allain, T.J., Heyderman, R.S., Russell, D.G., Mwandumba, H.C., 2014. Small alveolar macrophages are infected preferentially by HIV and exhibit impaired phagocytic function. *Mucosal Immunol.*, <http://dx.doi.org/10.1038/mi.2013.127>.
- Kang, B., Yu, D.-C., Chang, S.-Q., Chen, D., Dai, Y.-D., Ding, Y., 2008. Intracellular uptake, trafficking and subcellular distribution of folate conjugated single walled carbon nanotubes within living cells. *Nanotechnology* 19, 375103, <http://dx.doi.org/10.1088/0957-4484/19/37/375103>.
- Karve, S., Werner, M.E., Sukumar, R., Cummings, N.D., Copp, J.A., Wang, E.C., Li, C., Sethi, M., Chen, R.C., Pacold, M.E., Wang, A.Z., 2012. Revival of the abandoned therapeutic wortmannin by nanoparticle drug delivery. *Proc. Natl. Acad. Sci. U. S. A.* 109, 8230–8235, <http://dx.doi.org/10.1073/pnas.1120508109>.
- Karlson, T.D.L., Kong, Y.Y., Hardy, C.L., Xiang, S.D., Plebanski, M., 2013. The signalling imprints of nanoparticle uptake by bone marrow derived dendritic cells. *Methods* 60, 275–283, <http://dx.doi.org/10.1016/j.ymeth.2013.02.002>.
- Kastl, L., Sasse, D., Wulf, V., Hartmann, R., Mircheski, J., Ranke, C., Carregal-Romero, S., Martínez-López, J.A., Fernández-Chacón, R., Parak, W.J., Elsasser, H.-P., Rivera Gil, P., 2013. Multiple internalization pathways of polyelectrolyte multilayer capsules into mammalian cells. *ACS Nano* 7, 6605–66018, <http://dx.doi.org/10.1021/nn306032k>.
- Kettler, K., Veltman, K., van de Meent, D., van Wezel, A., Hendriks, A.J., 2014. Cellular uptake of nanoparticles as determined by particle properties, experimental conditions, and cell type. *Environ. Toxicol. Chem./SETAC* 33 (3), 481–492, <http://dx.doi.org/10.1002/etc.2470>.
- Khalil, I.A., Kogure, K., Akita, H., Harashima, H., 2006. Uptake pathways and subsequent intracellular trafficking in nonviral gene delivery. *Pharm. Res.* 58, 32–45, <http://dx.doi.org/10.1124/pr.58.1.8>.
- Kim, B.Y.S., Rutka, J.T., Chan, W.C.W., 2010. Nanomedicine. *N. Engl. J. Med.* 363, 2434–2443, <http://dx.doi.org/10.1056/NEJMra0912273>.
- Kim, J.A., Åberg, C., Salvati, A., Dawson, K.A., 2012. Role of cell cycle on the cellular uptake and dilution of nanoparticles in a cell population. *Nat. Nanotechnol.* 7, 62–68, <http://dx.doi.org/10.1038/nnano.2011.191>.
- Kirchhausen, T., Macia, E., Pelish, H.E., 2008. Use of dynasore, the small molecule inhibitor of dynamin, in the regulation of endocytosis. *Methods Enzymol.* 438, 77–93, [http://dx.doi.org/10.1016/S0076-6879\(07\)38006-3](http://dx.doi.org/10.1016/S0076-6879(07)38006-3).
- Kulkarni, S.A., Feng, S.-S., 2013. Effects of particle size and surface modification on cellular uptake and biodistribution of polymeric nanoparticles for drug delivery. *Pharm. Res.* 30, 2512–2522, <http://dx.doi.org/10.1007/s11095-012-0958-3>.
- Kumari, S., Mg, S., Mayor, S., 2010. Endocytosis unplugged: multiple ways to enter the cell. *Cell Res.* 20, 256–275, <http://dx.doi.org/10.1038/cr.2010.19>.
- Le Roy, C., Wrana, J.L., 2005. Clathrin- and non-clathrin-mediated endocytic regulation of cell signalling. *Nat. Rev. Mol. Cell Biol.* 6, 112–126, <http://dx.doi.org/10.1038/nrm1571>.
- Lemaire, J., Mkannez, G., Guerfali, F.Z., Gustin, C., Attia, H., Sghaier, R.M., Delagi, K., Laouini, D., Renard, P., 2013. MicroRNA expression profile in human

- macrophages in response to *Leishmania major* infection. PLoS Negl. Trop. Dis 7, e2478, <http://dx.doi.org/10.1371/journal.pntd.0002478>.
- Li, H., Li, Y., Jiao, J., Hu, H.-M., 2011. Alpha-alumina nanoparticles induce efficient autophagy dependent cross-presentation and potent antitumour response. Nat. Nanotechnol. 6, 645–650, <http://dx.doi.org/10.1038/nnano.2011.153>.
- Li, K., Schneider, M., 2014. Quantitative evaluation and visualization of size effect on cellular uptake of gold nanoparticles by multiphoton imaging-UV/Vis spectroscopic analysis. J. Biomed. Opt. 19, 101505, <http://dx.doi.org/10.1117/1.JBO.19.10.101505>.
- Liu, H., Chen, S., Zhou, Y., Che, X., Bao, Z., Li, S., Xu, J., 2013. The effect of surface charge of glycerol monooleate-based nanoparticles on the round window membrane permeability and cochlear distribution. J. Drug Target 21, 846–854, <http://dx.doi.org/10.3109/1061186X.2013.829075>.
- McMahon, H.T., Boucrot, E., 2011. Molecular mechanism and physiological functions of clathrin-mediated endocytosis. Nat. Rev. Mol. Cell Biol. 12, 517–533, <http://dx.doi.org/10.1038/nrm3151>.
- Moscatelli, A., Ciampolini, F., Rodighiero, S., Onelli, E., Cresti, M., Santo, N., Idilli, A., 2007. Distinct endocytic pathways identified in tobacco pollen tubes using charged nanogold. J. Cell Sci. 120, 3804–3819, <http://dx.doi.org/10.1242/jcs.012138>.
- Mu, Q., Hondow, N.S., Krzemiński, L., Brown, A.P., Jeuken, L.J.C., Routledge, M.N., 2012. Mechanism of cellular uptake of genotoxic silica nanoparticles. Part. Fibre Toxicol. 9, 29, <http://dx.doi.org/10.1186/1743-8977-9-29>.
- Nagahama, M., Itohayashi, Y., Hara, H., Higashihara, M., Fukutani, Y., Takagishi, T., Oda, M., Kobayashi, K., Nakagawa, I., Sakurai, J., 2011. Cellular vacuolation induced by *Clostridium perfringens epsilon*-toxin. FASEB J. 278, 3395–3407, <http://dx.doi.org/10.1111/j.1742-4658.2011.08263.x>.
- Olivier, M., Gregory, D.J., Forget, G., 2005. Subversion mechanisms by which *Leishmania* parasites can escape the host immune response: a signaling point of view. Clin. Microbiol. Rev. 18, 293–305, <http://dx.doi.org/10.1128/CMR.18.2.293-305.2005>.
- Olsson, A., 1995. Wortmannin, an inhibitor of phosphoinositide 3-kinase, inhibits transcytosis in polarized epithelial cells. J. Biol. Chem. 270, 28425–28432, <http://dx.doi.org/10.1074/jbc.270.47.28425>.
- Park, M.C., Kim, D., Lee, Y., Kwon, H.-J., 2013. CD83 expression induced by CpG-DNA stimulation in a macrophage cell line RAW 264.7. BMB Rep. 46, 448–453.
- Ponte-Sucre, A., Gulder, T., Wegehaupt, A., Albert, C., Rikanović, C., Schaelein, L., ... Frank, A., Schultheis, M., Unger, M., Holzgrabe, U., Bringmann, G., Moll, H., 2009. Structure-activity relationship and studies on the molecular mechanism of leishmanicidal N, C-coupled arylisoquinolinium salts. J. Med. Chem. 52, 626–636, <http://dx.doi.org/10.1021/jm801084u>.
- Rejman, J., Oberle, V., Zuhorn, I.S., Hoekstra, D., 2004. Size-dependent internalization of particles via the pathways of clathrin- and caveolae-mediated endocytosis. Biochem. J. 377, 159–169, <http://dx.doi.org/10.1042/BJ2003125>.
- Roth, M.G., 2007. Integrating actin assembly and endocytosis. Dev. Cell 13, 3–4, <http://dx.doi.org/10.1016/j.devcel.2007.06.005>.
- Saha, K., Kim, S.T., Yan, B., Miranda, O.R., Alfonso, F.S., Shlosman, D., Rotello, V.M., 2013. Surface functionality of nanoparticles determines cellular uptake mechanisms in mammalian cells. Small 9, 300–305, <http://dx.doi.org/10.1002/smll.201201129>.
- Sahay, G., Alakhova, D.Y., Kabanov, A.V., 2010. Endocytosis of nanomedicines. J. Control. Release 145, 182–195, <http://dx.doi.org/10.1016/j.jconrel.2010.01.036>.
- Salvati, A., Aberg, C., dos Santos, T., Varela, J., Pinto, P., Lynch, I., Dawson, K.A., 2011. Experimental and theoretical comparison of intracellular import of polymeric nanoparticles and small molecules: toward models of uptake kinetics. Nanomedicine 7, 818–826, <http://dx.doi.org/10.1016/j.nano.2011.03.005>.
- Sandvig, K., Pust, S., Skotland, T., van Deurs, B., 2011. Clathrin-independent endocytosis: mechanisms and function. Curr. Opin. Cell Biol. 23, 413–420, <http://dx.doi.org/10.1016/j.ceb.2011.03.007>.
- Sanjuan, M.A., Dillon, C.P., Tait, S.W.G., Moshiach, S., Dorsey, F., Connell, S., Komatsu, M., Tanaka, K., Cleveland, J.L., Withoff, S., Green, D.R., 2007. Toll-like receptor signalling in macrophages links the autophagy pathway to phagocytosis. Nature 450, 1253–1257, <http://dx.doi.org/10.1038/nature06421>.
- Sato, K., Nagai, J., Mitsui, N., Ryoko Yumoto, Takano, M., 2009. Effects of endocytosis inhibitors on internalization of human IgG by Caco-2 human intestinal epithelial cells. Life Sci. 85, 800–807, <http://dx.doi.org/10.1016/j.lfs.2009.10.012>.
- Scita, G., Di Fiore, P.P., 2010. The endocytic matrix. Nature 463, 464–473, <http://dx.doi.org/10.1038/nature08910>.
- Shima, F., Uto, T., Akagi, T., Baba, M., Akashi, M., 2013. Size effect of amphiphilic poly( $\gamma$ -glutamic acid) nanoparticles on cellular uptake and maturation of dendritic cells in vivo. Acta Biomater. 9, 8894–8901, <http://dx.doi.org/10.1016/j.actbio.2013.06.010>.
- Smith, D.M., Simon, J.K., Baker, J.R., 2013. Applications of nanotechnology for immunology. Nat. Rev. Immunol. 13, 592–605, <http://dx.doi.org/10.1038/nri3488>.
- Steigerwald, M., Moll, H., 2005. *Leishmania major* modulates chemokine and chemokine receptor expression by dendritic cells and affects their migratory capacity. Infect. Immun. 73, 2564–2567, <http://dx.doi.org/10.1128/IAI.73.4.2564-2567.2005>.
- Underhill, D.M., Goodridge, H.S., 2012. Information processing during phagocytosis. Nat. Rev. Immunol. 12, 492–502, <http://dx.doi.org/10.1038/nri3244>.
- Utaisincharoen, P., Kespichayawattana, W., Anuntagool, N., Chaisuriya, P., Pichyangkul, S., Krieg, a.M., Sirisinha, S., 2003. CpG ODN enhances uptake of bacteria by mouse macrophages. Clin. Exp. Immunol. 132, 70–75.
- Vercauteren, D., Vandebroucke, R.E., Jones, A.T., Rejman, J., Demester, J., De Smedt, S.C., Sanders, N.N., Braeckmans, K., 2010. The use of inhibitors to study endocytic pathways of gene carriers: optimization and pitfalls. Mol. Ther. 18, 561–569, <http://dx.doi.org/10.1038/mt.2009.281>.
- Wang, A.Z., Langer, R., Farokhzad, O.C., 2012. Nanoparticle delivery of cancer drugs. Annu. Rev. Med. 63, 185–198, <http://dx.doi.org/10.1146/annurev-med-040210-162544>.
- Wang, J., Huang, W.-L., Liu, R.-Y., 2009. CpG-ODN enhances ingestion of apoptotic neutrophils by macrophages. Clin. Exp. Med. 9, 37–43, <http://dx.doi.org/10.1007/s10238-008-0017-x>.
- Xia, T., Kovochich, M., Liong, M., Zink, J.I., Nel, A.E., 2008. Cationic polystyrene nanosphere toxicity depends on cell-specific endocytic and mitochondrial injury pathways. ACS Nano 2, 85–96, <http://dx.doi.org/10.1021/nn700256c>.
- Xu, S., Olenyuk, B.Z., Okamoto, C.T., Hamm-Alvarez, S.F., 2013. Targeting receptor-mediated endocytotic pathways with nanoparticles: rationale and advances. Adv. Drug Deliv. Rev 65, 121–138, <http://dx.doi.org/10.1016/j.addr.2012.09.041>.
- Yan, Y., Such, G.K., Johnston, A.P.R., Best, J.P., Caruso, F., 2012. Engineering particles for therapeutic delivery: prospects and challenges. ACS Nano 6, 3663–3669, <http://dx.doi.org/10.1021/nn3016162>.